INTERFACE

rsif.royalsocietypublishing.org

Research

Cite this article: Feix T, Kivell TL, Pouydebat E, Dollar AM. 2015 Estimating thumb–index finger precision grip and manipulation potential in extant and fossil primates. *J. R. Soc. Interface* **12**: 20150176.
http://dx.doi.org/10.1098/rsif.2015.0176

Received: 26 February 2015
Accepted: 23 March 2015

Subject Areas:
biomechanics, computational biology, bioengineering

Keywords:
grasping, *Australopithecus*, Neanderthal, manipulation, kinematic model, primates

Author for correspondence:
Thomas Feix
e-mail: thomas.feix@yale.edu

†These authors contributed equally to the study.

Electronic supplementary material is available at http://dx.doi.org/10.1098/rsif.2015.0176 or via http://rsif.royalsocietypublishing.org.

THE ROYAL SOCIETY PUBLISHING

Estimating thumb–index finger precision grip and manipulation potential in extant and fossil primates

Thomas Feix[1,†], Tracy L. Kivell[2,3,†], Emmanuelle Pouydebat[4] and Aaron M. Dollar[1]

[1]Department of Mechanical Engineering and Materials Science, Yale University, 9 Hillhouse Avenue, New Haven, CT 06511, USA
[2]Animal Postcranial Evolution Laboratory, School of Anthropology and Conservation, University of Kent, Marlowe Building, Canterbury CT2 7NR, UK
[3]Department of Human Evolution, Max Planck Institute for Evolutionary Anthropology, Deutscher Platz 6, Leipzig 04103, Germany
[4]Département d'Ecologie et de Gestion de la Biodiversité, UMR 7179 CNRS/MNHN, 57 rue Cuvier, Case postale 55, 75231 Paris Cedex 5, France

Primates, and particularly humans, are characterized by superior manual dexterity compared with other mammals. However, drawing the biomechanical link between hand morphology/behaviour and functional capabilities in non-human primates and fossil taxa has been challenging. We present a kinematic model of thumb–index precision grip and manipulative movement based on bony hand morphology in a broad sample of extant primates and fossil hominins. The model reveals that both joint mobility and digit proportions (scaled to hand size) are critical for determining precision grip and manipulation potential, but that having either a long thumb or great joint mobility alone does not necessarily yield high precision manipulation. The results suggest even the oldest available fossil hominins may have shared comparable precision grip manipulation with modern humans. In particular, the predicted human-like precision manipulation of *Australopithecus afarensis*, approximately one million years before the first stone tools, supports controversial archaeological evidence of tool-use in this taxon.

1. Introduction

Enhanced manual grasping is considered to have been a key adaptation separating the earliest primates from other early mammals [1,2]. This ability continued to evolve among primates to become most refined in humans; co-evolving with bipedalism, tool-use, brain enlargement and language [1–7]. Compared with other primates, the anatomy of the human hand helps to facilitate unique abilities, including forceful precision pinch grips between the pad of the thumb and the pads of the fingers and precision handling (manipulating objects within one hand) [3,5]. These dexterous abilities and associated anatomy are traditionally considered to have evolved in response to removing the hands from the constraints of locomotion as well as the mechanical demands of intensive tool-use and tool-production in our fossil hominin ancestors [3,5,8,9]. However, there is still much debate about the inferred manipulative capabilities of early fossil hominins, particularly with regard to tool-use [10–16] and potential subtle differences in precision grip movement or ability between Neanderthals and modern humans [17–19]. Furthermore, other primates, with markedly different hand morphology (e.g. hand proportions, thumb mobility) compared with that of humans, are also capable of using several different precision grips, including tip-to-tip or tip-to-side of the finger precision grips (rather than pad-to-pad as in humans), as well as in-hand movements [20], especially during feeding, tool-use [21–34] or experimental tool-making activities [35,36]. Unlike humans, the hands of other primates

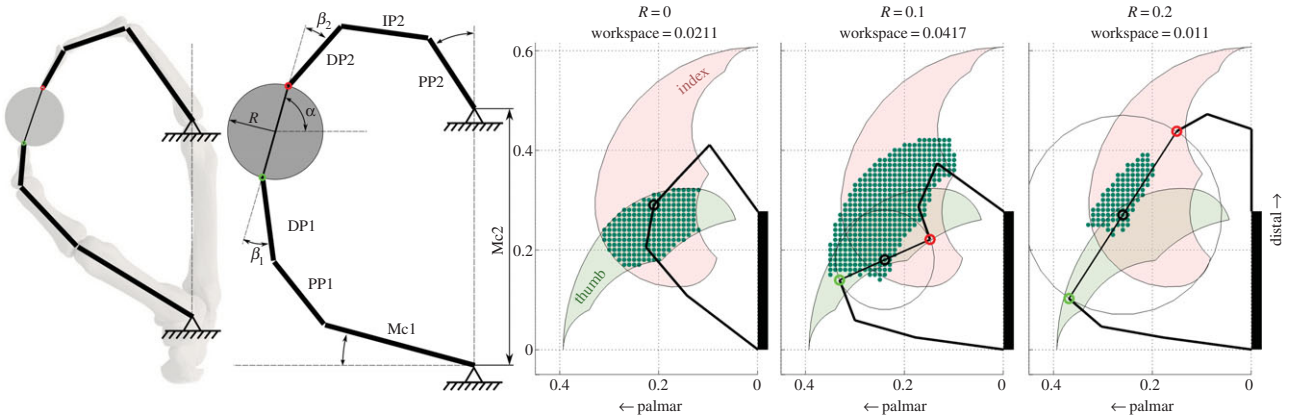

Figure 1. The thumb and index finger kinematic model. The model is based on three thumb segments (first metacarpal (Mc1), proximal phalanx (PP1) and distal phalanx (DP1)) and four index finger segments (Mc2, PP2, second intermediate phalanx (IP2) and DP2) of associated hand specimens. The digits touch a circular object of varying size (R, radius) and rotation (α). The relative orientation of the fingertips, touching two opposing points at the object, is β_1 (thumb) and β_2 (index finger). The area in which the object can be manipulated is then calculated. The three rightmost pictures show an example workspace (WS) of one representative human for three object sizes. In those pictures, one feasible configuration between the digits and object for each object size is shown. The dots represent the object positions for which a feasible configuration exists and therefore indicate the WS area. The shaded areas represent the positions the tip of thumb (green) and index (red) finger. (Online version in colour.)

must balance the morphological and functional requirements of locomotion, feeding and manipulation, all of which vary tremendously across the order Primates. From an evolutionary standpoint, this prompts several questions about if and how primate grasping is derived from the requirements associated with feeding and/or locomotor behaviour, what grasping abilities are unique to humans and when these evolved, and what morphological constraints might limit precision grasping.

These questions are not fully understood in part because previous studies on primate grasping—and specifically precision grasping—have focused on digit posture (e.g. contact between the hand and the object; [21,22,30]) or morphology (e.g. length of the thumb relative to the fingers; [3–5,9]), both of which have been difficult to link directly to dynamic digit movement. Furthermore, investigation of the evolution of grasping is limited to inferences from bony morphology only, as this is all that is preserved in the fossil record [10,14,37]. Experimental studies, including the kinematics [38], electromyography of muscle use [8] or force experienced by the digits [39] during particular grasping tasks provide important information about the biomechanics of grasping, but may not be logistically or ethically feasible on extant primates and cannot be applied to extinct taxa. A lack of methods enabling the quantification of digit movement and dexterity directly from bony morphology has limited our understanding of evolution and variation of precision manipulation in primates.

Among the wide range of grip types within the primate grasping repertoire, the thumb–index finger pinch is particularly important for increased manual dexterity [3,40]. Nearly all forms of precision grip and many power grips [41] involve thumb–index opposition, making it the foundation of stable human grasping of small objects. Furthermore, thumb–index opposition was critical for tool-related behaviours in human evolutionary history [42] and remains crucial in modern humans for many precision manipulation tasks (e.g. handwriting, fine scraping) and nearly all types of human in-hand manipulation (where a grasped object is positioned by moving the fingers) [43]. It also provides the greatest range of in-hand manipulation workspace (WS) compared with grasps with more than two digits [44].

This study presents a novel method founded in mechanism kinematics that allows us to estimate the precision manipulation capabilities between the thumb (first ray) and index finger (second ray) across a broad sample of extant primates and fossil hominins. Here, we use 'precision grip/grasp' to refer to a specific static thumb–index finger posture in which an object is held between the fingertips, whereas 'precision manipulation' reflects the active *movement* of objects held between the fingertips and generally requires complex individual digit control. The kinematic hand model is based on the segment (i.e. metacarpal and phalanges) lengths of the thumb and index finger from associated hand skeletons and inferred or measured mobility (i.e. range of motion) of the first and second ray joints [45] (figure 1). In particular, the model incorporates inferred variation in trapeziometacarpal joint mobility across major primate clades (e.g. opposable versus pseudo-opposable thumbs). The manipulation WS of a given hand is calculated as the area over which the fingers can position a circular object of varying size while satisfying the mechanical constraints of the model (see Material and methods). Thus, WS is a measure of dynamic thumb–index manipulation, providing insights into both the range of locations over which an object can be grasped by the thumb and index finger, as well as the space over which the grasped object can be actively positioned by those digits after being grasped. As such, we consider a hand with a larger thumb–index finger manipulation WS to be one with a greater precision grip potential and overall increased dexterity than a hand with a smaller manipulation WS. Niewoehner *et al.* [19] used a similar method to investigate precision grip ability in the Neanderthal hand. However, our method differs from this previous study by employing a full kinematic analysis quantifying for the first time the manipulation WS. Furthermore, as our analysis is completely automated, we were able to apply the method to a large comparative sample, rather than qualitatively comparing a Neanderthal to a modern human.

We apply this kinematic model to an extant primate sample, including $n = 360$ associated hand specimens from

38 species of extant hominoids, Old World and New World monkeys and strepsirrhines, and a fossil hominin sample comprising specimens with associated and complete thumb and index fingers that span nearly four million years of hominin evolution. The fossil hominin sample includes the Pliocene fossil hominin *Australopithecus afarensis* composite hand [10,11], Pleistocene fossil hominins *Australopithecus sediba* MH2 [14], *Homo neanderthalensis* Kebara 2 [46], and early *Homo sapiens* Qafzeh 9 [47] and Ohalo II H2 [48]. Although this kinematic model simplifies the complexity of anatomy and movement in the primate hand, and particularly that of the thumb, this simplicity makes the model applicable to associated fossil specimens for which knowledge about joint movements, soft-tissue anatomy or possibly other bones (e.g. carpals) is unknown. This model offers for the first time a method of assessing manipulative movement within the hand based on bony morphology alone. It can help to establish new links between behavioural studies and morphology, and may reveal potential manipulative capabilities in taxa for which behavioural or biomechanical studies have not yet been done (e.g. most strepsirrhines) or are not possible (i.e. fossil taxa and kinematic studies of most extant non-human primates). Here, we focus on the thumb–index finger movement of several extant primate taxa known for their dexterity (precision grip ability, manipulative skills or tool use) and fossil hominins. The model can be applied to extant and fossil primate and non-primate taxa alike, and can be modified to include different grips or ranges and planes of motion in future biomechanical studies.

Using this kinematic model, we predict that humans will have the largest thumb–index finger WS across all object sizes and that non-human primate taxa considered to be most dexterous in the wild and/or captivity—specifically African apes, baboons, macaques and capuchin monkeys—will have higher WS values than other primates [22,23,25–31]. We expect *Pongo* to have a different WS from other dexterous species because, although they are also adept tool-users, they have short thumbs and often use a variety of finger-only and non-hand (e.g. mouth or foot) strategies to grasp and use tools [24,30,49]. Among fossil taxa, we hypothesize that *Au. afarensis* will have a smaller thumb–index finger WS than *Au. sediba* and later *Homo*, and that *Au. sediba* will group with later *Homo* because of its long thumb [14]. We further predict that *H. neanderthalensis* will have distinct WS pattern, though not necessarily smaller, compared with early and recent *H. sapiens* owing to differences in relative segment lengths of the thumb [17].

2. Material and methods

2.1. Extant sample

Our dataset consists of 360 associated hand specimens from 38 primate species (figure 4 and electronic supplementary material, table S2), including hominoids, Old World monkeys, New World monkeys and several species of strepsirrhines (sexes pooled). The human sample includes African, European and small-bodied Khoisan individuals, all of which have very similar relative segment length proportions. Interarticular (IA) length of the first and second metacarpals and maximum length of the proximal, intermediate and distal phalanges of the first and second rays were measured on associated osteological specimens (i.e. instead of using species means for each segment). For part ($n = 230$) of the sample that did not have IA length for the metacarpals, total length (TL) was used to estimate IA length using regression based on $n = 130$ specimens (electronic supplementary material, figure S4)

$$\mathrm{IA}_{Mc1} = 0.964 \cdot \mathrm{TL}_{Mc1} \quad (R^2 = 0.998)$$
$$\mathrm{IA}_{Mc2} = 0.965 \cdot \mathrm{TL}_{Mc2} \quad (R^2 = 0.997).$$

The high correlation allowed transformation of TL measurements to IA length without the introduction of significant error. Associated specimens with at least one segment outside a $\pm 2.5\sigma$ range were removed from further analyses. This included the removal of five *H. sapiens*, two *P. pygmaeus*, two *Macaca fascicularis*, two *Loris tardigradus*, two *Tarsius syrichta*, one *Microcebus murinus* and one *Nycticebus coucang* individuals.

2.2. Fossil sample

Thumb and index finger segment lengths were measured directly from the fossils (electronic supplementary material, table S2). The *Au. afarensis* (3.9–2.9 Ma) composite hand is comprised fossils that are not associated with the same individual [10,11], and thus, there is debate regarding the hand proportions in this taxon and the potential for human-like precision grip [10,11,15,16,50]. However, we include *Au. afarensis* as an estimate of the potential primitive condition in hominins. Specimens included in the model are: Mc1 AL333w-39, PP1 AL333–69 and DP1 AL33–159 for the thumb, and Mc2 AL333–48, PP2 AL333–93, IP2 AL333–32 and DP2 is a mean length of the only two non-pollical distal phalanges, AL333w-11 and -50.

Australopithecus sediba (1.98 Ma) MH2 is the only (published) almost complete hand of early fossil hominin individual, and its morphology demonstrates a mosaic of primitive, African ape-like features and derived, human-like features [14]. MH2 is missing the distal phalanx of the index finger (DP2). Therefore, two models of *Au. sediba* were constructed estimating the length of the DP2 based on both a ratio of IP2/DP2 length in *Pan troglodytes* and in *H. sapiens*.

2.3. The kinematic model

The thumb and index finger are each modelled as a three link model, such that the basal joint is the trapeziometacarpal joint in the thumb and the metacarpophalangeal (McP) joint in the index finger (figure 1). The model and calculations are done in Matlab (MathWorks Inc., Natick, MA). The segment lengths are derived from the associated osteological hand specimens, but act as kinematic link lengths in the model. Thus, the joint centres are located at the end of the bone in the model, whereas in reality, the joints centres are located in the centre of the epiphyses.

It is assumed that the carpometacarpal joints of the thumb and index finger derive from a single point in morphospace, even though morphologically they are separated (Mc1 articulates with the trapezium, whereas the Mc2 articulates with the trapezoid and capitate in a more distal and medial anatomical position). Thus, the assumed distance between the trapeziometacarpal joint and the McP joint of the index finger is the IA length of the Mc2.

The thumb and index finger are restricted to movement in a single plane, even though the primary plane of movement for both digits is not coplanar. All joints are decoupled (i.e. can function independently), and each joint has one degree of freedom, acting as a hinge joint in flexion and extension only. Thus, abduction and adduction of the thumb and other out-of-the-plane movements are not modelled. Primates vary strongly in the morphology of the trapeziometacarpal joint and range of mobility. Therefore, the limit of movement for this joint follows the group mean estimations of flexion by Rose [45] for *Homo*

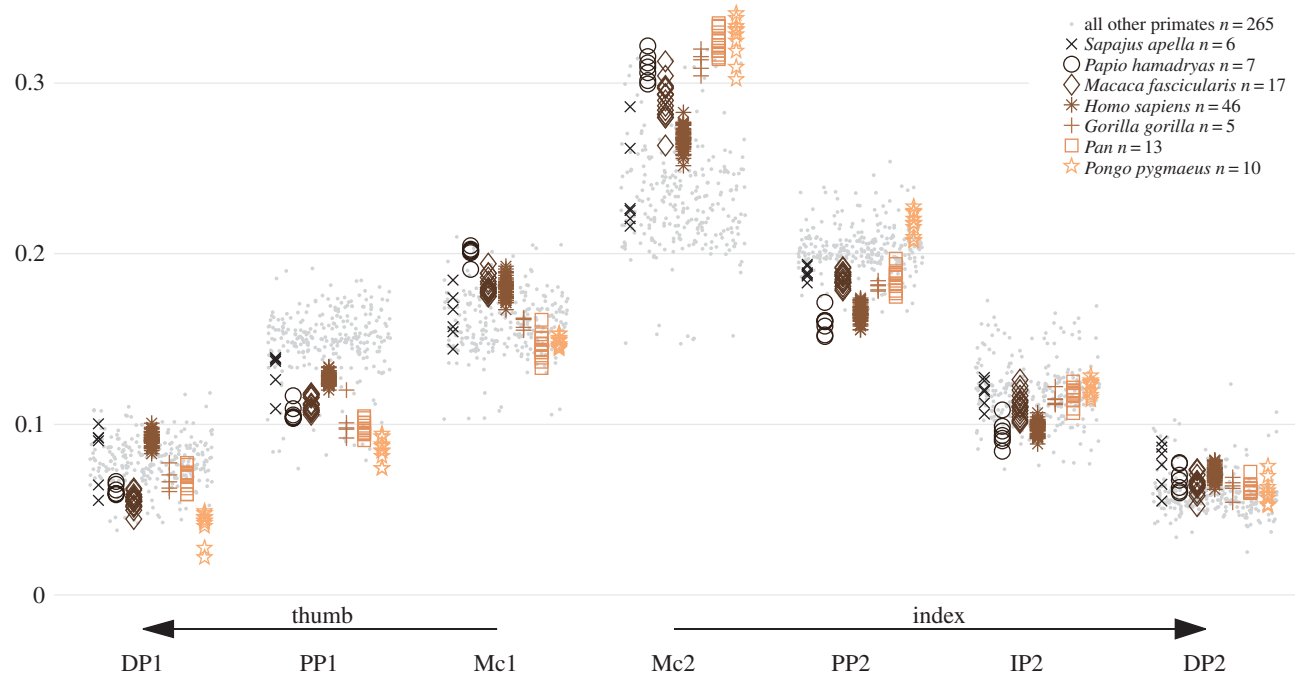

Figure 2. Relative segment lengths of the thumb and index finger in extant primates. The sum of all segments within each specimen is scaled to 1. The *Pan* sample includes both chimpanzees and bonobos combined, as digit proportions were very similar between the two species. The *H. sapiens* sample includes African, European and small-bodied Khoisan individuals. (Online version in colour.)

(37.6°), great apes (32.8°), cercopithecoids (21.4°), colobines (12.5°), New World monkeys (10.6°) and strepsirrhines (10.6°). The same value was used for all species within the respective groups. Although these values are estimated from the bony morphology [45], they are measured in a variety of different primate species and incorporate important differences in opposable (hominoids and Old World monkeys) and pseudo-opposable (New World monkeys and strepsirrhines) thumb mobility across the breadth of our sample [4]. The limit of movement for all other joints is based by necessity on the maximum range of motion in human joints, because this information is not known for all non-human primates. Maximum flexion values for the index finger are 85.5°, 102° and 72° for the McP, first interphalangeal joint (IPJ), and second IPJ, respectively [51]. In the thumb, maximum flexion of the McP is 59° and the IPJ is 67° [52].

In the kinematic model, the digits move to grip a circular object (figure 2) that varies in size, with a radius (scaled to hand size) of $R = 0$ (i.e. where the thumb and index finger touch) to $R = 0.3$. The object sizes are scaled to the size of the hand, such that a radius of 1 is equal to the TL of rays 1 and 2. Only a single point on the fingertip can contact to the object, the digits must oppose each other perfectly on the object (i.e. 180° apart on the object), and the digit and object must be non-intersecting (i.e. collisions limit the range of motion). When both digits are fully extended (i.e. straight), the angle between them is 90°. The relative angle β between the diameter connecting the grasp points and the distal finger segments (DP1, DP2) is restricted to $[-90 \ldots 90]$ degrees.

Soft tissues and muscle forces are not considered nor does the model take into account muscular and neural couplings between finger joints (which are not known or available for the majority of the specimens considered); this model is purely kinematic. Therefore, whether it is biologically possible for a given hand to apply forces in a particular direction, whereas grasping the object in a given configuration is not tested. However, the simplicity of the model makes it applicable to fossil specimens for which only information about bony morphology is preserved. Human joint ranges of motion were used for all joints of the fossil *H. sapiens* and *H. neanderthalensis* specimens, because overall hand morphology is generally very similar [18]. Given the mosaic human-like and *Pan*-like morphology of *Au. afarensis* and *Au. sediba* hands, two models were created for each; one using a *Pan* joint limit for the trapeziometacarpal joint and human joint limits for the remaining joints, and the other using a human limits for all joints.

2.4. Workspace calculation

To determine the area over which an object can be manipulated, a circular object is placed into the model. The object has two grasping points: index finger (red dot) and thumb (green dot; figure 1). The parameters of the object are the centre location $\mathbf{p} \in R^2$ and orientation (α). Furthermore, for each object position the relative orientation of fingertip and object (β_1 and β_2) can be varied. For a given object location $\mathbf{p}$, there are infinite object rotations α and hand configurations defined by β_1 and β_2. In order to count an object position $\mathbf{p}$ as valid, only one set of α, β_1 and β_2 that results in a feasible configuration (where both fingertips are able to touch their respective grasping points and each joint is within its defined limits) is necessary. Multiple solutions for one position will not give an additional benefit in the WS calculation.

For the actual calculation, the plane is discretized into equally spaced points, where the interpoint distance in x- and y-directions is dx. A smaller distance results in a finer grid, which leads to a higher precision of the WS calculation. For the actual WS calculations, dx is set to 0.01. For each location in the WS, the object is rotated between $\alpha = 0$–360°. In our case, one revolution of the object is discretized into 120 steps. Furthermore, the relative angle between object and finger is varied, $\beta_i = -90°$ to 90°. Those angles are discretized into the same number of bins as α. For each of those configurations ($\mathbf{p}$, α, β_1, β_2), it is checked whether a feasible finger configuration exists. Overall, the sum of all object positions $\mathbf{p}$, where at least one valid grasp configuration of α and β was found will determine the hand WS.

$$\mathrm{WS} = \mathrm{d}x^2 \sum_{i}^{N} a_i, \quad \text{where } a_i = \begin{cases} 1, & \exists \text{ valid grasp for any } \alpha, \beta_1, \beta_2 \\ 0, & \text{otherwise} \end{cases}$$

We look at a large diversity of primates that vary greatly in hand morphology and body mass. To facilitate comparison of hands of

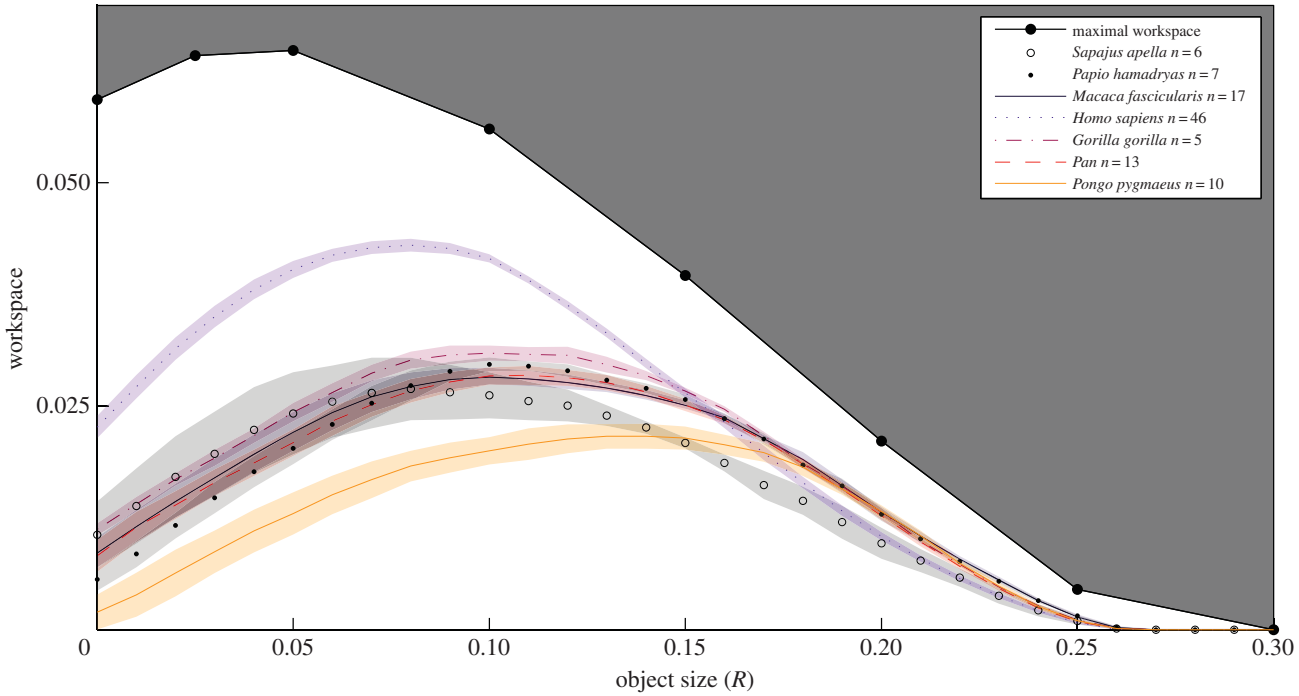

Figure 3. Workspace (WS) values relative to object size in a sample of extant primates. The bold lines or symbols represent the mean value for each taxon and the lightly shaded areas represent the standard deviation. The maximal WS line represents the highest achievable WS for each object size and was determined by finding the combination of segment lengths that resulted in the highest possible WS. *H. sapiens* have a much larger WS for smaller objects while *Pongo* has the smallest WS for most of the object sizes. All taxa generally have a similar WS for objects greater than $R = 0.2$. (Online version in colour.)

widely different sizes, all of the thumb and index finger segment lengths for each individual are normalized to a common length of 1

$$Mc1 + PP1 + DP1 + Mc2 + PP2 + IP2 + DP2 = 1.$$

This is the most straightforward normalization, as it relies only on parameters that are used for modelling the hand, as body mass is not known for most osteological specimens.

3. Results

3.1. Relative segment lengths in extant primates

A key morphology that has been linked to precision grip ability is the length of the thumb relative to the fingers [3,5]. The broad comparative primate sample we have collected here demonstrates substantial variation in thumb-to-index finger length ratio and the relative segment lengths within each ray (figure 2). Within the index finger, most of the variation across primates is in the length of the metacarpal and proximal phalanx, whereas all segments within the thumb vary strongly. Humans are distinct among primates in having the longest thumb relative to their index finger, which facilitates the ability to oppose the pad of the thumb to the distal digits and provides greater control of an object during precision handling [3–5]. However, other primates show a variety of different thumb–index finger proportions to accommodate requirements of locomotion or feeding, including reduced thumb length (e.g. *Presbytis*), reduced index finger length (e.g. *Loris*), elongated finger length (e.g. *Pan*, *Hylobates*) or reduced metacarpals, but elongated phalanges (e.g. *Daubentonia*; figure 2 and electronic supplementary material, figure S1) [4,53,54]. The primate taxa documented as being particularly dexterous during feeding or tool-use also vary greatly in their thumb–index finger proportions (figure 2). At one extreme, *Pongo* and less so *Pan* have a relatively long index finger and short thumb, whereas at the other extreme, *Papio* and less so *Sapajus*, show the opposite proportions with a relatively long thumb and are more similar to *H. sapiens* in this way. This variation in relative segment lengths has biomechanical consequences for thumb–index finger opposition.

3.2. Thumb–index finger workspace in extant primates

The precision grip WS for each individual and each taxon was calculated for grasping and manipulating a circular object varying in size (scaled to hand size) from $R = 0$ to 0.3, increasing incrementally by 0.01 (figure 1). The WS for $R = 0$ corresponds to the area over which the tips of the thumb, and the index finger can touch. As the size of the object increases up to $R = 0.3$, the WS increases until a point when the object size becomes a constraint on digit movement. The WS for all primates was zero for objects with an $R > 0.3$ (about the size of a ripe cantaloupe for the average human hand). Figure 1 shows an example WS for a representative human. The general behaviour is similar for all primate taxa, but the y-intersect and the maximum height and position vary for each individual and species.

Figure 3 and table 1 show the average and peak precision manipulation WS relative to object size in a sample of primate taxa that vary substantially in their locomotor and feeding behaviours, relative digit/segment lengths or inferred trapeziometacarpal joint mobility (figures 2 and 4 and electronic supplementary material, figure S2; also see Material and methods). Across all samples, humans have the largest WS for all objects with an $R < 0.15$ (slightly larger than a tennis ball for the average human hand; figure 3). The peak human WS is substantially higher and at a smaller object size ($R = 0.08$) than those of all other primates (table 1 and electronic supplementary material, table S1). Within non-human primates, *Gorilla* have the closest WS to humans, followed by *Pan* (including both chimpanzees and bonobos), but the peak WS for all African apes is at a much larger

Table 1. Position of the peak workspace and object size for a sample of extant and fossil primate taxa. The real object size corresponds to the object size that is achieved by scaling the relative object size back to real world units. Australopith 'human' and '*Pan*' refer to use of human versus *Pan* trapeziometacarpal joint range of motion in two separate kinematic models. In *Au. sediba* MH2, the length of the DP2 was also inferred using both human and *Pan* DP2/IP2 proportions (see Material and methods).

Taxon	peak workspace	relative object size (*R*)	real object size *R* (mm)
haplorhines			
Homo sapiens	0.043	0.08	19.00
Pan paniscus	0.029	0.11	28.70
P. troglodytes	0.028	0.10	26.2
Gorilla gorilla	0.031	0.10	28.70
Pongo pygmaeus	0.022	0.14	37.50
Hylobates lar	0.027	0.11	2.20
Papio hamadryas	0.030	0.10	15.60
Macaca fascicularis	0.028	0.10	10.00
Macaca mulatta	0.028	0.10	11.40
Presbytis cristata	0.016	0.16	18.00
Sapajus apella	0.027	0.08	7.90
Cebus albifrons	0.029	0.08	8.70
Alouatta semiculus	0.029	0.08	11.50
Tarsius bancanus	0.023	0.11	5.80
strepsirrhines			
Lepilemur leucopus	0.029	0.08	4.00
Propithecus verreauxi	0.029	0.09	9.60
Avahi laniger	0.024	0.11	7.40
Euoticus elegantulus	0.031	0.09	4.20
Loris tardigradus	0.029	0.09	2.90
Nycticebus coucang	0.030	0.09	4.00
Daubentonia madagascariensis	0.029	0.08	10.00
fossils			
early *H. sapiens* Qafzeh 9	0.044	0.08	2.90
early *H. sapiens* Ohalo II H2	0.042	0.07	2.50
H. neanderthalensis Kebara 2	0.043	0.08	3.00
Au. sediba MH2 (human)	0.044	0.08	2.10
Au. sediba MH2 (*Pan*)	0.040	0.09	2.40
Au. afarensis comp (human)	0.042	0.08	2.40
Au. afarensis comp (*Pan*)	0.040	0.08	2.40

object size than that of humans. *Papio* and *Macaca* mean and peak WS is broadly similar to that of *Pan*, both being slightly better at manipulating mid-sized objects but slightly less adept with very small or very large objects, despite a substantially different thumb–index finger ratio (figures 2 and 3) and lower trapeziometacarpal joint mobility (see Material and methods). *Sapajus* shows a large range of intraspecific variation (as reflected in the segment lengths in figure 2), but its peak WS is for relatively small objects and its overall WS is generally similar to *Gorilla* for manipulating smaller objects even though *Sapajus* has more limited thumb mobility. However, *Sapajus* falls below African apes, *Papio* and *Macaca* in manipulating larger objects ($R > 0.07$). *Pongo*, with a relatively short thumb, has a much smaller WS than all other taxa, apart from manipulating relatively large objects ($R > 0.18$; electronic supplementary material, figure S2).

Across our primate sample, there are some general patterns in precision manipulation WS despite differences in thumb–index finger proportions and joint mobility (figure 4). Although there is large variation in WS for small object sizes up to about $R = 0.1$, manipulation WS generally converges across all primates, including humans, for the larger $R > 0.15$ objects (figure 4). In general, all taxa show their greatest WS with a relative object size of around $R = 0.1$, whereas manipulation of objects with an $R = 0$ is similar or smaller to the WS of $R = 0.2$ objects. The only exceptions to this general primate pattern are humans (and fossil hominins, see below), New World monkeys (*Cebus*, *Alouatta* and with some overlap,

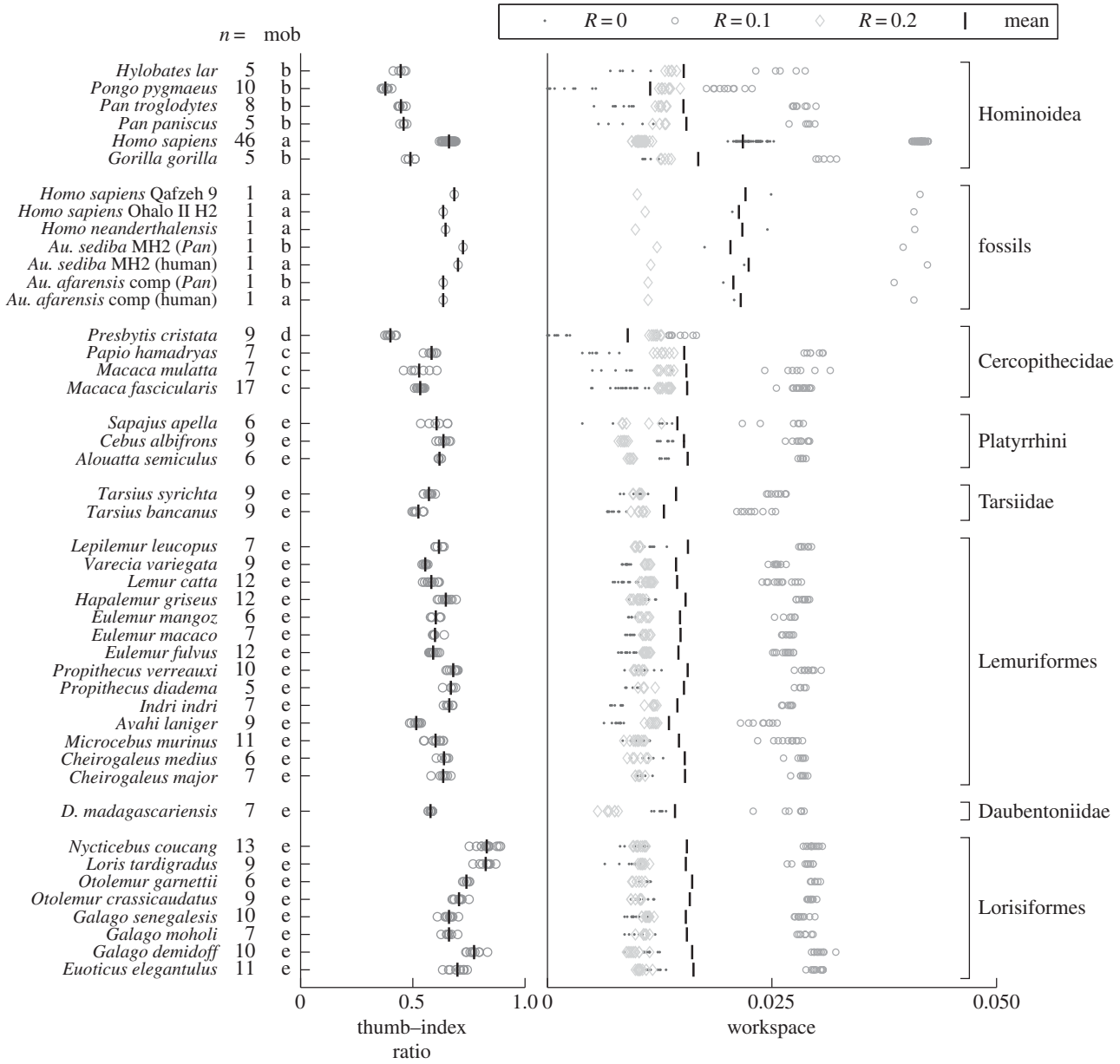

Figure 4. Thumb–index finger proportion and workspace (WS) values for three objects sizes across the comparative extant and fossil primate sample. Left plot shows a ratio of thumb length to index finger length and the right plot shows the WS values for object sizes $R = 0$ (in which thumb and index finger are touching), $R = 0.1$ and $R = 0.2$. The vertical line represents the mean, and the symbols represent the results for each individual for the respective object sizes. The 'mob' column indicates mobility of the trapeziometacarpal joint according to Rose [45], where $a = 37.6$, $b = 32.8$, $c = 21.4$, $d = 12.5$ and $e = 10.6^{\circ}$.

Sapajus) and aye-ayes (*Daubentonia*), in which the WS for $R = 0$ is substantially greater than that of $R = 0.2$.

These results highlight the enhanced human ability to precision grasp small objects, but also reveal that different combinations of relative thumb–index finger proportions and joint mobility can produce similar manipulation capabilities (figure 4 and electronic supplementary material, figure S2).

3.3. Thumb–index finger proportions and manipulation workspace in fossil hominins

While there are some subtle differences, fossil hominin finger proportions, manipulation WS values all fall within the range of recent *H. sapiens* variation (figure 4). Australopith hands demonstrate a combination of *Pan*-like and human-like morphology and thus inferring mobility of the thumb is challenging. Therefore, we created two models each for *Au. afarensis* and *Au. sediba* using either a *Pan*-like or human-like trapeziometacarpal range of motion (see Material and methods). Furthermore, the *Au. afarensis* composite hand is based on unassociated fossils from multiple individuals, and thus this study presents only one possible estimate of precision manipulation in this taxon. The *Au. afarensis* thumb–index proportions here are generally similar to those of *H. sapiens* but with a slightly longer index finger (figure 4; electronic supplementary material, figure S3). In contrast, the associated MH2 hand of *Au. sediba* demonstrates a relatively long thumb, particularly the first metacarpal, compared with other fossil hominins and recent *H. sapiens* (figure 4 and electronic supplementary material, figure S3) [14]. Despite this variation in morphology and mobility, the mean manipulation WS for all *Au. afarensis* and *Au. sediba* thumb and index finger kinematic models fall within the recent *H. sapiens* range of variation. Using a *Pan*-like range of trapeziometacarpal mobility, both australopiths fall slightly below the mean and peak WS of *H. sapiens* and *H. neanderthalensis*, especially

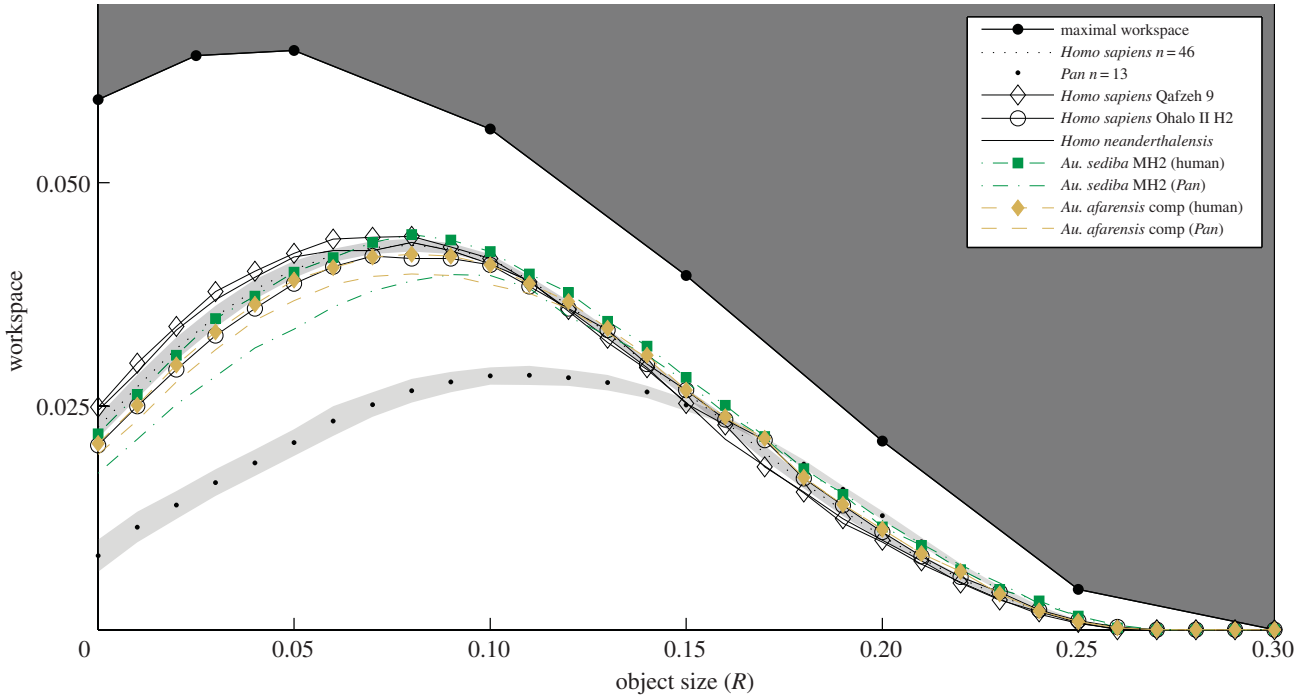

Figure 5. Workspace (WS) values relative to object size in fossil hominins compared with extant *Pan* and *H. sapiens*. The bold lines and symbols represent the mean value for each taxon and the lightly shaded areas for *Pan* and *H. sapiens* represent the standard deviation. The maximal WS line represents the highest achievable WS for each object size and was determined by finding the combination of segment lengths that resulted in the highest possible WS. All fossil hominins have a larger WS for smaller objects ($R < 0.15$) compared with *Pan*. Using *Pan*-like trapeziometacarpal mobility, *Au. afarensis* composite hand and *Au. sediba* have a lower WS than fossil and extant *Homo*, but with human-like mobility are similar to these taxa. All taxa generally have a similar WS for objects greater than $R = 0.15$. (Online version in colour.)

for small objects ($R < 0.1$; figure 5 and table 1). When using a human-like range of trapeziometacarpal mobility, *Au. afarensis* has the same mean and peak manipulation WS as recent *H. sapiens*, whereas *Au. sediba* falls out slightly higher than recent *H. sapiens* and fossil *Homo*, in particular for object sizes $R > 0.08$.

Given their generally recent human-like morphology, all *H. neanderthalensis* and early *H. sapiens* kinematic models used a recent human range of motion at the trapeziometacarpal joint. However, compared with recent *H. sapiens*, some fossil *Homo* specimens demonstrate subtle differences in thumb–index finger proportions (figure 4 and electronic supplementary material, figure S3). *H. neanderthalensis* demonstrate distinct pollical proportions with a relatively longer pollical distal phalanx but shorter proximal phalanx [17]. Early *H. sapiens* Qafzeh 9 has a relatively longer thumb than Ohalo II H2, although both fall within the range of variation of recent *H. sapiens* (figure 4). Despite these differences, all fossil *Homo* generally have a similar mean and peak manipulation WS for a relatively small object size, although *H. neanderthalensis* and early *H. sapiens* Qafzeh 9 have slightly higher WSs for very small objects ($R > 0.05$; figure 5).

Overall, there is little variation in the potential thumb–index finger WS across australopiths (especially using human range of mobility), fossil *Homo*, and recent *H. sapiens* despite subtle differences in thumb–index finger proportions and potential thumb mobility.

4. Discussion

This study models, for the first time, digit movement during precision grasping and manipulation in a broad sample of humans, non-human primates and fossil hominins. Our kinematic thumb–index finger model allows one to assess tip-to-tip precision manipulation potential from the bony morphology of associated hand skeletons. This model is largely based (by necessity of available data) on human kinematics, and thus likely provides the most realistic estimate of digit movement in humans and fossil hominins, while perhaps overestimating or underestimating precision grip potential in non-human primates (see Material and methods). Although the model incorporates variation in thumb mobility (e.g. opposable versus pseudo-opposable thumbs), it does not incorporate the complexity of additional planes of motion (e.g. abduction–adduction), muscle and tendon function, or neurological and myological couplings across segments or digits as these data are unknown for the vast majority of extant primates and are unavailable for fossil specimens. This model also does not take into consideration the associated cognitive or ecological factors that may be required for or promote particular grasping behaviours. The simplicity of the model, however, makes it ideal for comparative analyses across extant and fossil primate and/or non-primate taxa alike, and offers a novel method of assessing how variation in bony morphology can affect digit movement. With further research, the model can be adapted to include different ranges of motion in multiple planes and potentially different grasping behaviours (e.g. pad-to-pad or power grip) between the thumb, index finger or other fingers. Nevertheless, results from the current model provide support for our hypotheses and also reveal several general patterns in primate thumb–index finger precision manipulation potential, despite large variation in hand morphology.

Across our broad sample of primates, the highest manipulation WS for all taxa is for non-zero object sizes

when the tip of the thumb and index finger are not touching. The majority of primates demonstrate a similar WS pattern, in which maximal WS is generally between a relative object size of $R = 0.05$ and 0.15 (figure 4 and electronic supplementary material, figure S2). This similar pattern is also a consequence of the similarity of segment length proportions between primates, where many species have similar ratios between two adjacent segments. This 'sweet spot' around the maximal WS is a balance of trade-offs: grasping an object can be thought of as extending the length of the digit by the object radius to increase the WS size, but as the object gets larger relative to the size of the hand, it begins to collide and interfere with digit movement. Across primates, different combinations of thumb–index finger proportions and joint mobility can provide a similar manipulation WS. For example, a relatively short thumb but high trapeziometacarpal joint mobility, as in African apes and *Hylobates*, yields similar WS values as a relatively long thumb and limited thumb mobility of many Lemuriformes and Lorisiformes [55]. Although the dexterity of great apes has been well documented [20–24,27,32], recent experimental studies suggest that the manipulative abilities in some strepsirrhines may be underestimated [56,57], and our results offer support for future research in these taxa. At the same time, these results also demonstrate that a relatively long thumb—a key morphological feature often linked to precision grip ability in extant and fossil apes [4,5,10,14,58]—does not necessarily translate into greater thumb–index finger manipulation. Although humans and fossil hominins have a higher manipulation WS, especially for smaller objects, several strepsirrhines, including *Propithecus* and most Lorisiformes, have a similar or higher thumb–index finger ratio compared with humans (owing to a markedly reduced length of the index finger), but substantially lower mean manipulation WS. However, the segment proportions of most non-human primates are at a biomechanical disadvantage relative to the human proportions, such that even with higher human-like trapeziometacarpal joint mobility, their WSs are substantially lower than that of humans. These results highlight the functional importance of joint mobility and a kinematic 'balance' in hand proportions.

Results from this kinematic model offer support for most of our hypotheses. First, we predicted that extant humans would have the largest thumb–index finger WS for all object sizes compared with other primates. Humans have a much higher mean and peak WS for small-to-medium objects (i.e. $R = 0.0$–0.15; $R = 0$–35 mm for an average human hand size) than all other extant primates. This is consistent with comparative biomechanical and behavioural studies highlighting the enhanced human ability to securely hold and manipulate small objects between the thumb and index finger [3,5,23,30]. However, humans have a slightly lower WS than other dexterous primates for larger objects (i.e. $R > 0.15$), suggesting that the human hand is particularly well suited to manipulate smaller objects (figure 3 and electronic supplementary material, figure S2). These results thus provide further empirical support for Napier's [3, p. 652] original observation that thumb–index finger precision grips are key to human manipulative abilities. Although our current model does not investigate the manipulative WS of pad-to-pad precision grips that are distinct to humans, it is interesting that even a tip-to-tip precision grip model—a grip that many other primates are capable of using—shows a potential optimization for smaller objects in humans relative to other taxa. As to why the human hand may have evolved to be particularly adept at manipulating small- and medium-sized objects may be related to a particular focus in our early evolutionary history on flake tool-use [12], food foraging or processing of small items similar to that of extant baboons [59], or any number of other manipulative behaviours [11,16]. We predict that modelling the distinctive pad-to-pad precision grip, in which the distal IPJ is extended rather than flexed, will further highlight the enhanced human ability to manipulate small objects in particular compared with other primates.

Second, we predicted that non-human primates traditionally considered more dexterous in the wild and/or captivity would have higher WS values than other non-human primates. This hypothesis is partially supported by the high mean WS in *Gorilla* and the high WS specifically for small objects in *Sapajus* (as well as *Cebus*). Although *Gorilla* do not regularly use tools in the wild like their chimpanzee cousins, they often use the thumb and index finger to grasp small objects [30,60] and exhibit a larger variety of precision grips during food preparation [27,60,61]. Similarly, *Sapajus* has evolved myological and neurological features that facilitate digit individualization [62] and a 'functionally' opposable thumb [26]. *Sapajus* exhibits considerable manipulative skills with small food items between the thumb and index finger, compared with the whole-hand grip strategies of other New World monkeys (i.e. *Saimiri* and *Saguinus*; [26,63,64]). Although *Sapajus* is more well known for its nut-cracking activities, these are done with large (i.e. 25% of their body mass) stone anvils that require bimanual power grips rather than precision grasping [65]. *Cebus* has a similarly high WS for small objects and is also known to manipulate leaves as tools in the wild [66]. However, *Alouatta* demonstrate similar WS values to *Sapajus* and *Cebus* and are not known to have enhanced manipulative skills in the wild or captivity (though this has not yet been studied). Furthermore, the other primates known to be particularly dexterous—*Pan*, *Papio* and *Macaca*—have the same mean and peak manipulation WS as the general 'primate' pattern (despite large variation in thumb–index proportions and joint mobility), which does not support our hypothesis that these taxa would have higher thumb–index finger manipulation than other primates. *Pongo*, as predicted, demonstrates a much lower mean and peak thumb–index finger WS compared with all other primates (except *Presbytis*) for small- and medium-sized objects ($R < 0.18$), which may help to explain why they often use within-finger grips or the mouth to manipulate objects [24,49] (electronic supplementary material, figure S2).

Third, we found general support for our predictions among the fossil taxa. Overall, all fossil australopiths and *Homo* fall within the range of variation in recent *H. sapiens* manipulation WS. Using either *Pan*-like or human-like trapeziometacarpal joint mobility, *Au. afarensis* mean thumb–index finger WS falls at or just slightly below the recent *H. sapiens* and fossil *Homo* means (figure 4). This study uses just one possible hand configuration for *Au. afarensis* with thumb–index finger proportions that are similar to recent *H. sapiens*. Other research has demonstrated that hand proportions in *Au. afarensis* may be more similar to *Gorilla* [15]. Furthermore, *Au. afarensis* Mc1 and trapezium articular morphology suggests that range of motion at this joint may have been more similar to *Pan* [50,67] and thus it is possible that *Au. afarensis* may have had a smaller thumb–index manipulation WS than later

hominins and was, in particular, less adept at manipulating small objects.

Using a *Pan*-like trapeziometacarpal joint mobility, *Au. sediba* falls below the recent and fossil *Homo* mean WS despite having a relatively longer thumb (figures 4 and 5; electronic supplementary material, figure S3). Like *Au. afarensis*, the *Pan*-like model for *Au. sediba* has a lower WS for manipulating small objects ($R < 0.1$), highlighting the importance of thumb mobility (rather than thumb length in this case) for fine-tuned precision manipulation (figure 5). However, the trapeziometacarpal morphology of the *Au. sediba* Mc1 indicates a larger range of mobility than *Au. afarensis* [14], suggesting that human-like *Au. sediba* model may be a better estimate of thumb–index manipulation in this early fossil hominin. Using human-like trapeziometacarpal mobility, *Au. sediba* has a slightly higher mean WS than recent *H. sapiens*, but generally has the same manipulation WS as recent and fossil *Homo*, as predicted. Nevertheless, the fact that the *Au. afarensis* and *Au. sediba* thumb–index manipulation potential falls generally within the *Homo* range of variation is consistent with previous suggestions that both australopiths may have been capable of at least some human-like precision grips [5,14,16,67]. This functional assessment is further supported by archaeological evidence of tool-use in *Au. afarensis*-bearing deposits at 3.4 Ma [12] and the first recognizable stone tools at approximately 2.6 Ma [68]. These results also suggest that *Au. afarensis* may have had greater dexterity than is required for cutting with a stone [32], including manipulative and tool-related behaviours that may not preserve in the archaeological record.

Finally, the results do not support for our prediction that *H. neanderthalensis* (represented here only by Kebara 2) will have distinct, though not necessarily smaller, manipulation WS pattern compared with early and recent *H. sapiens* owing to differences in relative segment lengths of the thumb [17]. *H. neanderthalensis* has a similar mean WS and identical peak WS for the same relatively small object size as that of recent *H. sapiens* (figure 4 and table 1). When WS is viewed across different object sizes, *H. neanderthalensis* falls above the recent *H. sapiens* WS range of variation for very small objects ($R < 0.05$; figure 5). However, early *H. sapiens* Qafzeh 9 displays a similar WS pattern suggesting that potential increase in thumb–index precision grip of small objects is not related to the distinct *H. neanderthalensis* thumb proportions. The inclusion of additional associated *H. neanderthalensis* hand skeletons is needed to test whether there is subtle, yet distinct, pattern in the manipulation WS compared with *H. sapiens*. For example, Niewoehner *et al.* [19] found that the thumb–index tip contact ability of Neandertal La Ferrassie I was similar to that of modern humans, but this similarity was not quantified.

These results derived from a broad sample of extant and fossil primates demonstrate that this kinematic model of thumb–index finger precision manipulation based on digit segment lengths provides a useful tool for assessing digit movement. This model provides the first opportunity to assess how variation in bony morphology and joint mobility can affect precision grip and precision manipulation. As such, it is applicable and adaptable to variety of extant and fossil tetrapod taxa for which manual (or pedal) grasping ability is of interest.

Data accessibility. The segment measurements that were collected by the authors have been uploaded as part of the electronic supplementary material.

Acknowledgements. We thank Dr Pierre Lemelin for generously sharing his data on extant strepsirrhines. We thank L. Berger, J. Kibii and B. Zipfel and the University of the Witwatersrand, W. Kimbel, G. Semishaw, G. Shimelies and the National Museum of Ethiopia, V. Volpato and Senckenberg Museum Frankfurt, and Y. Rak, I. Hershkovitz, D. Nadel and Tel Aviv University for access to fossil specimens, and F. Mayer, S. Jancke and the Museum für Naturkunde Berlin, C. Boesch, J.-J. Hublin and the Max- Planck-Institut für evolutionäre Anthropologie, S. Kirchengast and the Universität Wien, E. Gilissen, W. Wendelen and Musée royal de L'Afrique central, J. Moggi Cecchi, S. Bortoluzzi and the University of Florence, K. Zyskowski, L. Jones and the Yale Peabody Museum, S. King, S. Matarazzo and the University of Massachussetts Amherst, J. Chupasko and the Harvard Museum of Comparative Zoology, E. Westwig and the American Museum of Natural History, F. Zachos, A. Bibl and the Naturhistorisches Museum Wien for access to comparative extant material.

Funding statement. We are grateful for funding from the Gustavus and Louise Pfeiffer Research Foundation and the US National Science Foundation CAREER Award grant IIS-0953856 (AMD), and European Research Council Starting grant no. 336301 and Natural Sciences and Engineering Research Council of Canada (T.L.K.). We also thank the Action Transversale du Muséum National d'Histoire Naturelle: Formes possibles, Formes réalisées and Collections vivantes (Paris, France; E.P.).

Authors' contributions. E.P. and A.M.D. devised the analysis. T.F. and T.L.K. collected segment length data. T.F. created the model and figures. T.F. and T.L.K wrote the manuscript. All authors interpreted the results and edited the manuscript.

Competing interests. The authors declare no competing interests.

References

1. Wood Jones F. 1916 *Arboreal man*. London, UK: Edward Arnold.
2. Cartmill M. 1974 Rethinking primate origins. *Science* **184**, 436–443. (doi:10.1126/science.184.4135.436)
3. Napier JR. 1960 Studies of the hands of living primates. *Proc. Zool. Soc. London* **134**, 647–657. (doi:10.1111/j.1469-7998.1960.tb05606.x)
4. Napier JR. 1993 *Hands*. Princeton, NJ: Princeton University Press.
5. Marzke MW. 1997 Precision grips, hand morphology, and tools. *Am. J. Phys. Anthropol.* **102**, 91–110. (doi:10.1002/(SICI)1096-8644(199701)102:1<91::AID-AJPA8>3.0.CO;2-G)
6. Ehrsson HH, Fagergren A, Forssberg H. 2001 differential fronto-parietal activation depending on force used in a precision grip task: an fMRI study. *J. Neurophysiol.* **85**, 2613–2623.
7. Christiansen MH, Kirby S. 2003 Language evolution: consensus and controversies. *Trends Cogn. Sci.* **7**, 300–307. (doi:10.1016/S1364-6613(03)00136-0)
8. Marzke MW, Toth N, Schick K, Reece S, Steinberg B, Hunt K, Linscheid RL, An KN. 1998 EMG study of hand muscle recruitment during hard hammer percussion manufacture of Oldowan tools. *Am. J. Phys. Anthropol.* **105**, 315–332. (doi:10.1002/(SICI)1096-8644(199803)105:3<315::AID-AJPA3>3.0.CO;2-Q)
9. Tocheri MW, Orr CM, Jacofsky MC, Marzke MW. 2008 The evolutionary history of the hominin hand since the last common ancestor of *Pan* and *Homo*. *J. Anat.* **212**, 544–562. (doi:10.1111/j.1469-7580.2008.00865.x)
10. Marzke MW. 1983 Joint functions and grips of the *Australopithecus afarensis* hand, with special reference to the region of the capitate. *J. Hum. Evol.* **12**, 197–211. (doi:10.1016/S0047-2484(83)80025-6)
11. Alba DM, Moyà-Solà S, Köhler M. 2003 Morphological affinities of the *Australopithecus afarensis* hand on the basis of manual proportions and relative thumb length. *J. Hum. Evol.* **44**, 225–254. (doi:10.1016/S0047-2484(02)00207-5)

12. McPherron SP, Alemseged Z, Marean CW, Wynn JG, Reed D, Geraads D, Bobe R, Béarat HA. 2010 Evidence for stone-tool-assisted consumption of animal tissues before 3.39 million years ago at Dikika, Ethiopia. *Nature* **466**, 857–860. (doi:10.1038/nature09248)
13. Domínguez-Rodrigo M, Pickering TR, Bunn HT. 2011 Reply to McPherron *et al.*: Doubting Dikika is about data, not paradigms. Proc. Natl Acad. Sci. *USA* **108**, E117. (doi:10.1073/pnas.1104647108)
14. Kivell TL, Kibii JM, Churchill SE, Schmid P, Berger LR. 2011 *Australopithecus sediba* hand demonstrates mosaic evolution of locomotor and manipulative abilities. *Science* **333**, 1411–1417. (doi:10.1126/science.1202625)
15. Rolian C, Gordon AD. 2013 Reassessing manual proportions in *Australopithecus afarensis*. *Am. J. Phys. Anthropol.* **152**, 393–406. (doi:10.1002/ajpa.22365)
16. Almécija S, Alba DM. 2014 On manual proportions and pad-to-pad precision grasping in *Australopithecus afarensis*. *J. Hum. Evol.* **73**, 88–92. (doi:10.1016/j.jhevol.2014.02.006)
17. Trinkaus E, Villemeur I. 1991 Mechanical advantages of the Neanderthal thumb in flexion: a test of an hypothesis. *Am. J. Phys. Anthropol.* **84**, 249–260. (doi:10.1002/ajpa.1330840303)
18. Niewoehner WA. 2001 Behavioral inferences from the Skhul/Qafzeh early modern human hand remains. *Proc. Natl Acad. Sci. USA* **98**, 2979–2984. (doi:10.1073/pnas.041588898)
19. Niewoehner WA, Bergstrom A, Eichele D, Zuroff M, Clark JT. 2003 Digital analysis: manual dexterity in Neanderthals. *Nature* **422**, 395. (doi:10.1038/422395a)
20. Crast J, Fragaszy D, Hayashi M, Matsuzawa T. 2009 Dynamic in-hand movements in adult and young juvenile chimpanzees (*Pan troglodytes*). *Am. J. Phys. Anthropol.* **138**, 274–285. (doi:10.1002/ajpa.20925)
21. Boesch C, Boesch H. 1993 Different hand postures for pounding nuts with natural hammers by wild chimpanzees. In *Hands of primates* (eds H Preuschoft, D Chivers), pp. 31–43. Vienna, Australia: Springer.
22. Christel M. 1993 Grasping techniques and hand preferences in Hominoidea. In *Hands of primates* (eds H Preuschoft, D Chivers), pp. 91–108. Vienna, Australia: Springer.
23. Marzke MW, Wullstein KL. 1996 Chimpanzee and human grips: a new classification with a focus on evolutionary morphology. *Int. J. Primatol.* **17**, 117–139. (doi:10.1007/BF02696162)
24. Van Schaik CP, Fox EA, Sitompul AF. 1996 Manufacture and use of tools in wild Sumatran orangutans. *Naturwissenschaften* **83**, 186–188. (doi:10.1007/BF01143062)
25. Westergaard GC, Suomi SJ. 1997 Capuchin monkey (*Cebus apella*) grips for the use of stone tools. *Am. J. Phys. Anthropol.* **103**, 131–135. (doi:10.1002/(SICI)1096-8644(199705)103:1<131::AID-AJPA9>3.0.CO;2-Z)
26. Christel MI, Fragaszy D. 2000 Manual function in *Cebus apella*. Digital mobility, preshaping, and endurance in repetitive grasping. *Int. J. Primatol.* **21**, 697–719. (doi:10.1023/A:1005521522418)
27. Byrne RW, Corp N, Byrne JM. 2001 Manual dexterity in the gorilla: bimanual and digit role differentiation in a natural task. *Anim. Cogn.* **4**, 347–361. (doi:10.1007/s100710100083)
28. Gumert MD, Kluck M, Malaivijitnond S. 2009 The physical characteristics and usage patterns of stone axe and pounding hammers used by long-tailed macaques in the Andaman Sea region of Thailand. *Am. J. Primatol.* **71**, 594–608. (doi:10.1002/ajp.20694)
29. Macfarlane NBW, Graziano MSA. 2009 Diversity of grip in *Macaca mulatta*. *Exp. Brain Res.* **197**, 255–268. (doi:10.1007/s00221-009-1909-z)
30. Pouydebat E, Gorce P, Coppens Y, Bels V. 2009 Biomechanical study of grasping according to the volume of the object: human versus non-human primates. *J. Biomech.* **42**, 266–272. (doi:10.1016/j.jbiomech.2008.10.026)
31. Pouydebat E, Reghem E, Borel A, Gorce P. 2011 Diversity of grip in adults and young humans and chimpanzees (*Pan troglodytes*). *Behav. Brain Res.* **218**, 21–28. (doi:10.1016/j.bbr.2010.11.021)
32. Tonooka R, Matsuzawa T. 1995 Hand preferences of captive chimpanzees (*Pan troglodytes*) in simple reaching for food. *Int. J. Primatol.* **16**, 17–35. (doi:10.1007/BF02700151)
33. Haslam M *et al*. 2009 Primate archaeology. *Nature* **460**, 339–344. (doi:10.1038/nature08188)
34. McGrew WC. 2013 Is primate tool use special? Chimpanzee and New Caledonian crow compared. *Phil. Trans. R. Soc. Lond. B* **368**, 20120422. (doi:10.1098/rstb.2012.0422)
35. Toth N, Schick KD, Savage-Rumbaugh ES, Sevcik RA, Rumbaugh DM. 1993 Pan the tool-maker: investigations into the stone tool-making and tool-using capabilities of a bonobo (*Pan paniscus*). *J. Archaeol. Sci.* **20**, 81–91. (doi:10.1006/jasc.1993.1006)
36. Schick KD, Toth N, Garufi G, Savage-Rumbaugh ES, Rumbaugh D, Sevcik R. 1999 Continuing investigations into the stone tool-making and tool-using capabilities of a bonobo (*Pan paniscus*). *J. Archaeol. Sci.* **26**, 821–832. (doi:10.1006/jasc.1998.0350)
37. Napier J. 1962 The evolution of the hand. *Sci. Am.* **207**, 56–62. (doi:10.1038/scientificamerican1262-56)
38. Reghem E, Chèze L, Coppens Y, Pouydebat E. 2013 Unconstrained 3D-kinematics of prehension in five primates: lemur, capuchin, gorilla, chimpanzee, human. *J. Hum. Evol.* **65**, 303–312. (doi:10.1016/j.jhevol.2013.06.011)
39. Williams EM, Gordon AD, Richmond BG. 2012 Hand pressure distribution during Oldowan stone tool production. *J. Hum. Evol.* **62**, 520–532. (doi:10.1016/j.jhevol.2012.02.005)
40. Landsmeer JM. 1962 Power grip and precision handling. *Ann. Rheum. Dis.* **21**, 164–170. (doi:10.1136/ard.21.2.164)
41. Cutkosky MR. 1989 On grasp choice, grasp models, and the design of hands for manufacturing tasks. *Robot. Autom. IEEE Trans.* **5**, 269–279. (doi:10.1109/70.34763)
42. Marzke MW, Shackley MS. 1986 Hominid hand use in the pliocene and pleistocene: evidence from experimental archaeology and comparative morphology. *J. Hum. Evol.* **15**, 439–460. (doi:10.1016/S0047-2484(86)80027-6)
43. Bullock IM, Ma RR, Dollar AM. 2013 A hand-centric classification of human and robot dexterous manipulation. *Haptics, IEEE Trans.* **6**, 129–144. (doi:10.1109/toh.2012.53)
44. Bullock IM, Feix T, Dollar AM. 2014 Dexterous workspace of human two- and three-fingered precision manipulation. *IEEE Haptics Symp.*, 41–47. (doi:10.1109/HAPTICS.2014.6775431)
45. Rose MD. 1992 Kinematics of the trapezium-1st metacarpal joint in extant anthropoids and Miocene hominoids. *J. Hum. Evol.* **22**, 255–266. (doi:10.1016/0047-2484(92)90058-h)
46. Arensburg B *et al*. 1985 Une sépulture néandertalienne dans la grotte de Kébara (Israël). *Comptes-rendus des séances l'Académie des Sci. Série 2, Mécanique-physique, Chim. Sci. l'univers, Sci. la terre* **300**, 227–230.
47. Van der Meersch B. 1981 *Les hommes fossiles de Gafzeh*. Israël. *Les hommes fossiles de Gafzeh* (*Israël*). Paris, France: Centre National de la Recherche Scientifique.
48. Hershkovitz I, Speirs MS, Frayer D, Nadel D, Wish-Baratz S, Arensburg B. 1995 Ohalo II H2: a 19,000-year-old skeleton from a water-logged site at the Sea of Galilee, Israel. *Am. J. Phys. Anthropol.* **96**, 215–234. (doi:10.1002/ajpa.1330960302)
49. O'Malley RC, McGrew WC. 2000 Oral tool use by captive orangutans (*Pongo pygmaeus*). *Folia Primatol.* (*Basel*). **71**, 334–341. (doi:10.1159/000021756)
50. Bush ME, Lovejoy CO, Johanson DC, Coppens Y. 1982 Hominid carpal, metacarpal, and phalangeal bones recovered from the Hadar formation: 1974–1977 collections. *Am. J. Phys. Anthropol.* **57**, 651–677. (doi:10.1002/ajpa.1330570410)
51. Mallon WJ, Brown HR, Nunley JA. 1991 Digital ranges of motion: normal values in young adults. *J. Hand Surg. Am.* **16**, 882–887. (doi:10.1016/S0363-5023(10)80155-8)
52. Jenkins M, Bamberger H, Black L, Nowinski R. 1998 Thumb joint flexion. What is normal? *J.* Hand Surg. J. Br. Soc. Surg. Hand **23**, 796–797. (doi:10.1016/s0266-7681(98)80100-9)
53. Schultz AH. 1936 Characters common to higher primates and characters specific for man. *Q. Rev. Biol.* **11**, 259–283. (doi:10.1086/394508)
54. Jouffroy FK, Godinot M, Nakano Y. 1993 Biometrical characteristics of primate hands. In *Hands of primates* (eds H Preuschoft, D Chivers), pp. 133–171. Vienna, Austria: Springer.
55. Bishop A. 1964 Use of the hand in lower primates. In *Evolutionary and genetic biology of primates*, vol. 2 (ed. J Buettner-Janusch), pp. 133–225. New York, NY: Academic Press.
56. Schöneich S. 1993 Hand usage in the ring-tailed lemur (*Lemur catta* Linnaeus 1758) when solving manipulative tasks. In *Hands of primates* (eds H Preuschoft, D Chivers), pp. 7–20. Vienna, Austria: Springer.

57. Santos LR, Mahajan N, Barnes JL. 2005 How prosimian primates represent tools: experiments with two lemur species (*Eulemur fulvus* and *Lemur catta*). *J. Comp. Psychol.* **119**, 394–403. (doi:10.1037/0735-7036.119.4.394)
58. Moyà-Solà S, Köhler M, Rook L. 1999 Evidence of hominid-like precision grip capability in the hand of the Miocene ape *Oreopithecus*. *Proc. Natl Acad. Sci. USA* **96**, 313–317. (doi:10.1073/pnas.96.1.313)
59. Torigoe T. 1985 Comparison of object manipulation among 74 species of non-human primates. *Primates* **26**, 182–194. (doi:10.1007/bf02382017)
60. Pouydebat E, Berge C, Gorce P, Coppens Y. 2006 La préhension chez les Primates: précision, outils et perspectives évolutives. *C. R. Palevol.* **5**, 597–602. (doi:10.1016/j.crpv.2005.10.011)
61. Neufuss J, Deschner T, Robbins M, Pouydebat E, Kivell T. 2013 Hand use during non-locomotor behaviours in the wild African apes. *FOLIA Primatol.* **84**, 307.
62. Bortoff G, Strick P. 1993 Corticospinal terminations in two new-world primates: further evidence that corticomotoneuronal connections provide part of the neural substrate for manual dexterity. *J. Neurosci.* **13**, 5105–5118.
63. Costello MB, Fragaszy DM. 1988 Prehension in *Cebus* and *Saimiri*: I. Grip type and hand preference. *Am. J. Primatol.* **15**, 235–245. (doi:10.1002/ajp.1350150306)
64. Lemelin P, Grafton B. 1998 Grasping performance in *Saguinus midas* and the evolution of hand prehensility in primates. In *Primate locomotion* (eds E Strasser, J Fleagle, A Rosenberger, H McHenry), pp. 131–144. New York, NY: Springer.
65. Fragaszy DM, Visalberghi E, Fedigan LM. 2004 *The complete capuchin: the biology of the genus* Cebus. Cambridge, UK: Cambridge University Press.
66. Phillips KA. 1998 Tool use in wild capuchin monkeys (*Cebus albifrons trinitatis*). *Am. J. Primatol.* **46**, 259–261. (doi:10.1002/(SICI)1098-2345(1998)46:3<259::AID-AJP6>3.0.CO;2-R)
67. Tocheri MW, Marzke MW, Liu D, Bae M, Jones GP, Williams RC, Razdan A. 2003 Functional capabilities of modern and fossil hominid hands: three-dimensional analysis of trapezia. *Am. J. Phys. Anthropol.* **122**, 101–112. (doi:10.1002/ajpa.10235)
68. Semaw S, Renne P, Harris JWK, Feibel CS, Bernor RL, Fesseha N, Mowbray K. 1997 2.5-million-year-old stone tools from Gona, Ethiopia. *Nature* **385**, 333–336. (doi:10.1038/385333a0)

ELECTRONIC SUPPLEMENTARY MATERIAL

Title: Estimating thumb-index finger precision grip and manipulation potential in extant and fossil primates

Authors: Thomas Feix, Tracy L. Kivell, Emmanuelle Pouydebat, Aaron M. Dollar

Supplementary Figure 1. Relative segment lengths of the thumb and index finger in selected extant primates. The sum of all segments of one specimen is scaled to 1. Each species is colored differently and the grey dots in the background represent the full primate sample.

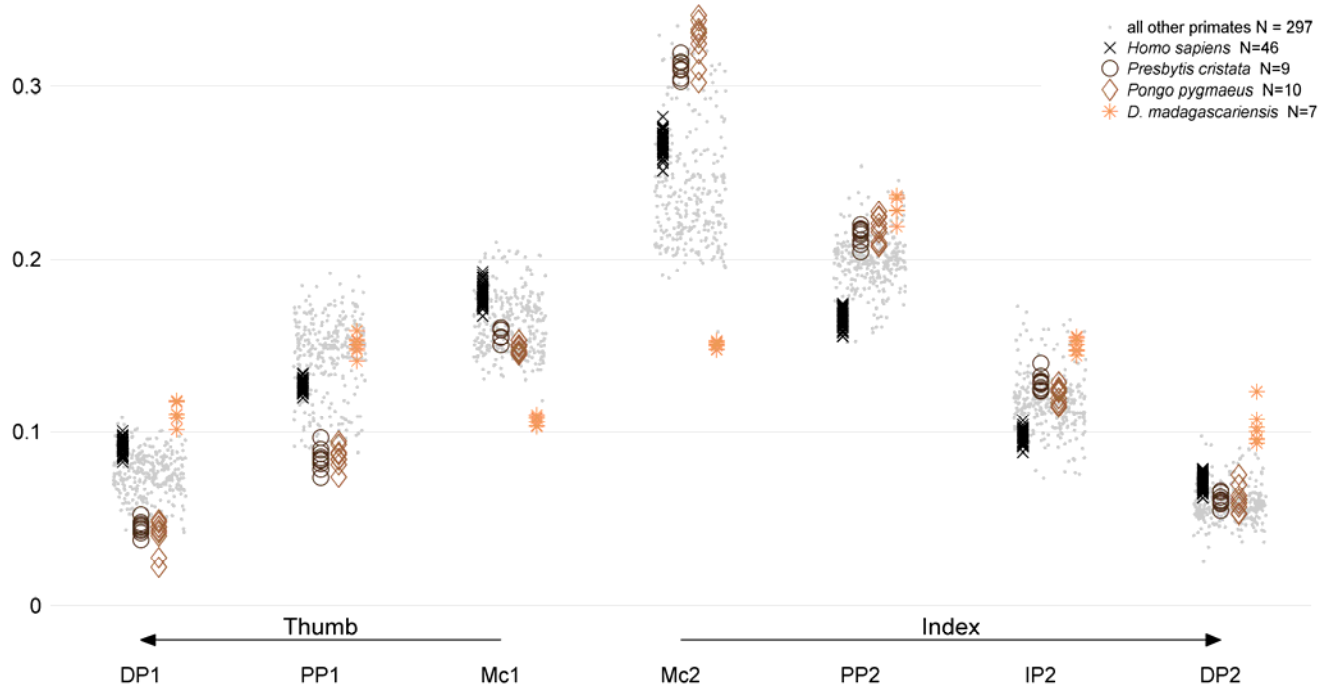

Supplementary Figure 2. Workspace values relative to object size in a sample of extant and extinct primates. The bold lines represent the mean value for each taxon and the lightly shades areas represent the standard deviation. The maximal workspace line represents the highest achievable workspace for each object size and was determined by finding the combination of segment lengths that resulted in the highest possible workspace. Humans and fossil hominins have a much higher workspace compared with all other primates. *Presbytis*, with a markedly reduced length of the index finger, has the lowest workspace values for a large range of object sizes (R=0-0.15). *Pongo* has also has a low thumb-index finger ratio due to a relatively long index finger, however, the larger range of motion at the trapeziometacarpal joint results in a slightly larger workspace than *Presbytis*. *Daubentonia* has the lowest workspaces for R > 0.15, but for smaller object sizes, the workspaces are well within the range of the primate sample. This atypical behavior is a direct consequence of its unique segment proportions, including a second metacarpal that is shorter than the second proximal phalanx.

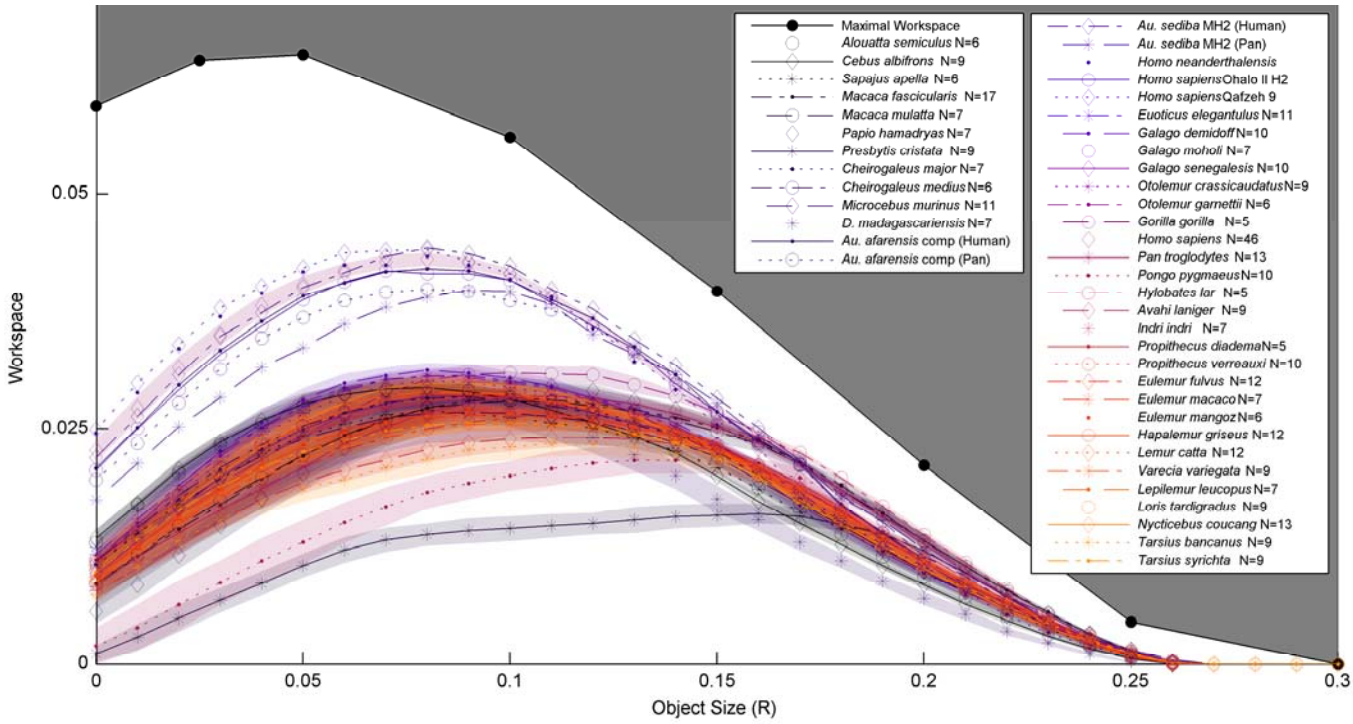

Supplementary Figure 3. Relative segment lengths of the thumb and index finger in extinct primates. The sum of all segments for of specimen is scaled to 1. The length of the missing DP2 in *Au. sediba* is estimated using the ratio of IP2/DP2 of *H. sapiens* (resulting in a longer DP2, with other segments relatively shorter) and *Pan* (resulting in a shorter DP2, with other segments relatively longer). The other segments of *Au. sediba* changed too as the sum of all segments is scaled to 1.

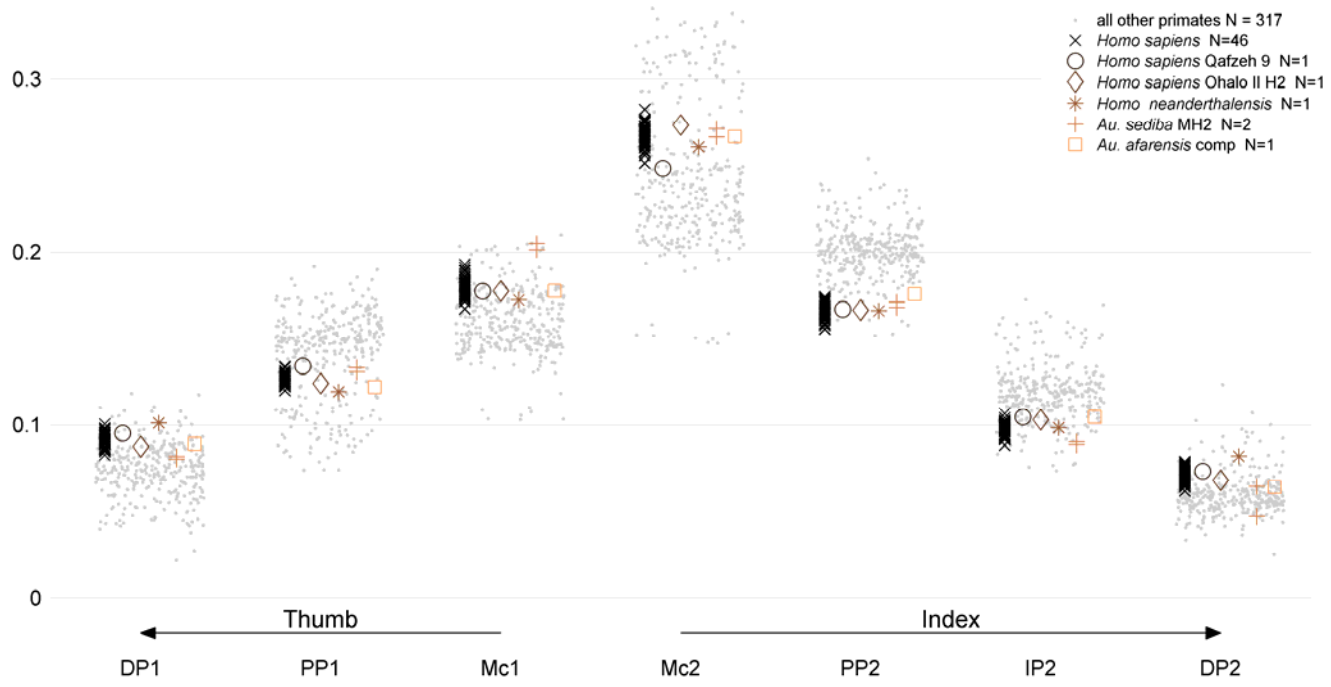

Supplementary Figure 4. Comparison of interarticular and total length for the metacarpal bones. A regression of first (above) and second (below) metacarpal interarticular length relative to total length. The regression line has a y-intersect at 0 and is fitted to all data points. The high correlation between these two variables means that total length can be used to infer the interarticular length with little error.

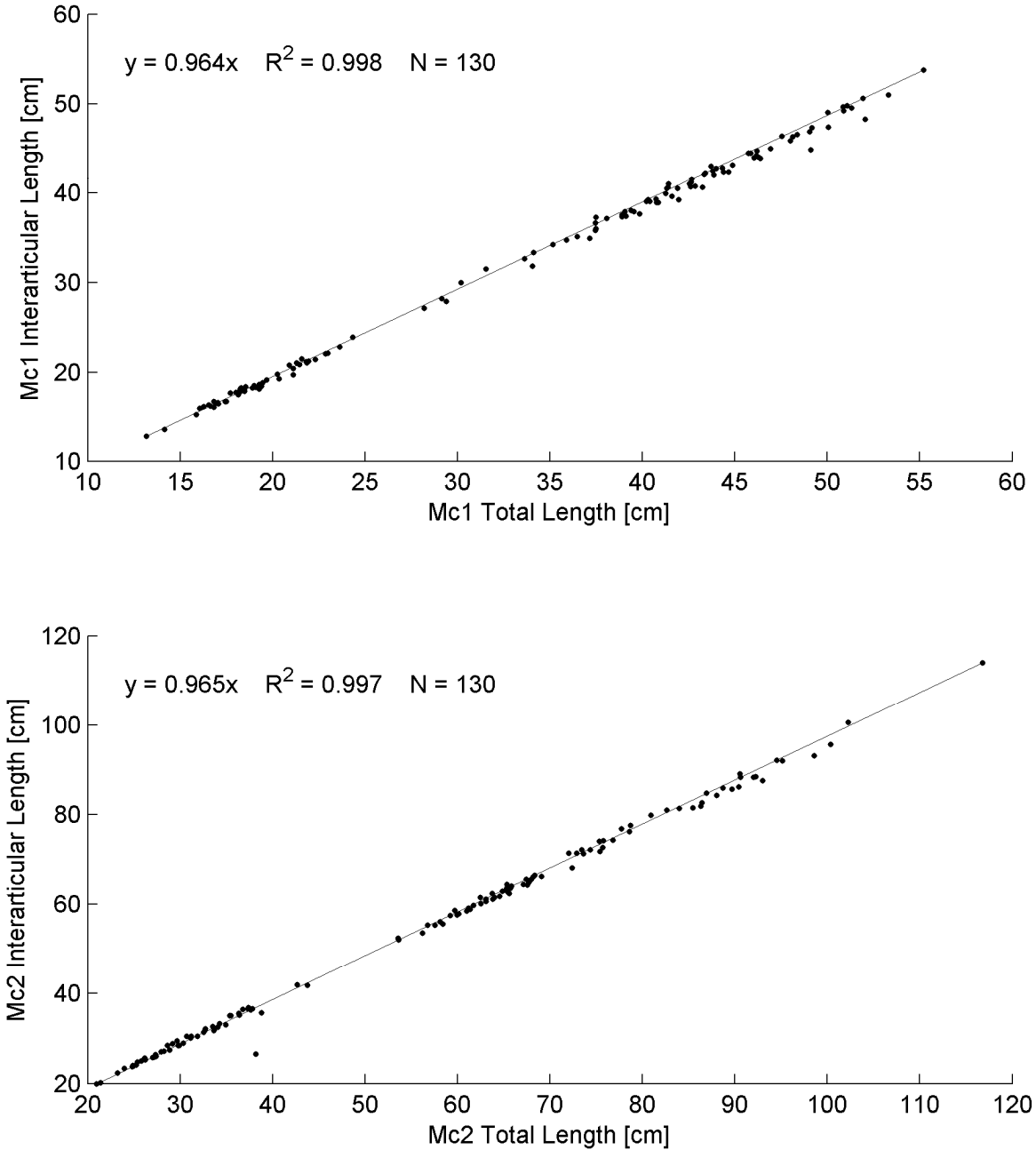

Supplementary Table 1. Position of the peak workspace and object size for the full comparative sample. The real object size corresponds to the object size that is achieved by scaling the relative object size back by to real world units. Australopith "human" and "*Pan*" refer to use of human versus *Pan* trapeziometacarpal joint range of motion in two separate kinematic models. In *Au. sediba* MH2, the length of the DP2 was also inferred using human versus *Pan* DP2/IP2 proportions (see Materials and Methods).

Group	Species	N	peak workspace	relative object size (R)	real object size R (mm)
Hominoidea	*Hylobates lar*	5	0.027	0.11	22.2
	Pongo pygmaeus	10	0.022	0.14	37.5
	Pan troglodytes	8	0.028	0.1	26.2
	Pan paniscus	5	0.029	0.11	28.6
	Homo sapiens	46	0.043	0.08	19
	Gorilla gorilla	5	0.031	0.1	28.7
Fossils	*early H. sapiens* Qafzeh 9	1	0.044	0.08	2.9
	early H. sapiens Ohalo II H2	1	0.042	0.07	2.5
	H. neanderthalensis	1	0.043	0.08	3
	Au. sediba MH2 (Pan)	1	0.04	0.09	2.4
	Au. sediba MH2 (Human)	1	0.044	0.08	2.1
	Au. afarensis comp (Pan)	1	0.04	0.08	2.4
	Au. afarensis comp (Human)	1	0.042	0.08	2.4
Cercopithecidae	*Presbytis cristata*	9	0.016	0.16	18
	Papio hamadryas	7	0.03	0.1	15.6
	Macaca mulatta	7	0.028	0.1	11.4
	Macaca fascicularis	17	0.028	0.1	10
Platyrrhini	*Sapajus apella*	6	0.027	0.08	7.9
	Cebus albifrons	9	0.029	0.08	8.7
	Alouatta semiculus	6	0.029	0.08	11.5
Tarsiidae	*Tarsius syrichta*	9	0.026	0.09	4.3
	Tarsius bancanus	9	0.023	0.11	5.8
Lemuriformes	*Lepilemur leucopus*	7	0.029	0.08	4
	Varecia variegata	9	0.026	0.1	10.6
	Lemur catta	12	0.026	0.09	6.8
	Hapalemur griseus	12	0.029	0.09	5.1
	Eulemur mangoz	6	0.027	0.09	6.5
	Eulemur macaco	7	0.027	0.09	7.5
	Eulemur fulvus	12	0.026	0.09	7
	Propithecus verreauxi	10	0.029	0.09	9.6
	Propithecus diadema	5	0.028	0.09	12.4
	Indri indri	7	0.027	0.1	17.7
	Avahi laniger	9	0.024	0.11	7.4
	Microcebus murinus	11	0.027	0.09	2
	Cheirogaleus medius	6	0.028	0.09	2.7
	Cheirogaleus major	7	0.028	0.09	3.9
	D. madagascariensis	7	0.029	0.08	10
Lorisiformes	*Nycticebus coucang*	13	0.03	0.09	4
	Loris tardigradus	9	0.029	0.09	2.9
	Otolemur garnettii	6	0.031	0.08	4.4
	Otolemur crassicaudatus	9	0.03	0.08	4.3
	Galago senegalesis	10	0.028	0.08	2.5
	Galago moholi	7	0.029	0.08	2.5
	Galago demidoff	10	0.031	0.08	2.1
	Euoticus elegantulus	11	0.031	0.09	4.2

Supplementary Table 2. Raw segment length measurement data for selected species. All units of the segment measurements (Mc1, PP1, DP1, Mc2, PP2, IP2, DP2) are in mm and the museum keys are as follows: AMNH: American Museum of Natural History New York, HMNH: Harvard Museum of Natural History, YPM: Yale Peabody Museum, UM-APC: University of Massachusetts Amherst, ZMB: Museum für Naturkunde Berlin, NMW: Naturhistorisches Museum Wien, UV: University of Vienna, UNI-Fl: University of Florence, MRAC: Musée royal de L'Afrique central, SMF: Senckenberg Museum Frankfurt, NME: National Museum of Ethiopia, WITS: University of this Witwatersrand, TAU: Tel Aviv University

Group	Species	Key	Mc1	PP1	DP1	Mc2	PP2	IP2	DP2
Platyrrhini	*Alouatta semiculus*	AMNH 23330	21.1	21.4	12.6	30.1	30.3	18.8	10.2
	Alouatta semiculus	AMNH 23334	21.1	19.8	12.5	28.4	28.7	18.8	11.1
	Alouatta semiculus	AMNH 23337	18.6	19.5	11.8	25.8	26.9	17.3	9.8
	Alouatta semiculus	AMNH 23335	21.5	19.3	12.6	28.5	28.6	17.4	10.4
	Alouatta semiculus	AMNH 23329	22.8	21.8	13.2	31.3	31.2	19.7	11.5
	Alouatta semiculus	AMNH 14660	22.0	23.3	14.8	32.0	32.2	20.5	12.7
	Cebus albifrons	AMNH 15485	18.9	14.5	10.4	25.9	19.4	12.4	10.3
	Cebus albifrons	AMNH 23403	16.7	14.3	9.6	23.9	18.3	12.4	9.4
	Cebus albifrons	AMNH 23401	18.0	15.9	12.0	23.4	21.2	13.5	10.7
	Cebus albifrons	AMNH 23399	18.3	16.7	10.8	24.7	21.7	14.3	9.9
	Cebus albifrons	AMNH 15484	15.3	13.5	10.0	23.8	18.1	12.3	10.0
	Cebus albifrons	AMNH 200753	16.7	14.4	10.4	24.0	19.8	13.5	9.8
	Cebus albifrons	AMNH 14017	17.8	16.0	10.7	24.1	21.7	13.8	9.7
	Cebus albifrons	AMNH 201434	13.6	12.2	7.7	19.9	16.5	11.2	6.8
	Cebus albifrons	AMNH 201288	18.3	16.3	10.9	25.0	20.2	13.7	10.0
	Sapajus apella	AMNH 188037	16.6	13.6	9.1	22.4	18.1	11.8	7.6
	Sapajus apella	AMNH 95129	16.7	15.0	9.8	24.0	20.3	13.8	9.0
	Sapajus apella	AMNH 80169	12.9	12.4	8.2	20.2	16.8	10.7	8.1
	Sapajus apella	HMNH 61405	17.7	10.5	5.3	27.4	18.6	10.2	6.2
	Sapajus apella	YPM MAM 7577	17.0	12.3	6.3	25.5	18.8	12.3	5.4
	Sapajus apella	YPM MAM 6873	15.9	14.0	10.2	21.9	19.1	11.4	8.8
Cercopithecidae	*Macaca fascicularis*	UM-APC 217	18.0	10.9	5.8	31.7	19.0	10.8	5.3
	Macaca fascicularis	UM-APC 281	19.8	11.6	6.3	31.7	19.3	10.7	7.1
	Macaca fascicularis	HMNH 35611	20.4	11.3	5.2	32.0	19.3	10.7	6.3
	Macaca fascicularis	HMNH 35612	19.7	12.8	6.1	32.5	20.3	12.2	7.2
	Macaca fascicularis	HMNH 35656	18.5	12.3	5.8	30.4	18.6	11.4	6.6
	Macaca fascicularis	HMNH 35658	16.3	9.5	4.5	25.7	15.8	9.0	5.6
	Macaca fascicularis	HMNH 35694	16.3	10.0	5.3	27.2	17.1	10.4	6.1
	Macaca fascicularis	HMNH 35729	17.9	11.0	6.3	30.4	19.5	10.5	6.4
	Macaca fascicularis	HMNH 35727	16.1	9.6	5.0	27.1	17.1	10.4	5.9
	Macaca fascicularis	HMNH 35736	19.2	10.9	5.9	28.9	18.1	12.2	6.5
	Macaca fascicularis	HMNH 35735	16.6	10.6	5.0	25.3	17.1	10.5	5.3
	Macaca fascicularis	HMNH 37349	16.2	10.9	5.3	26.0	17.8	10.2	6.1
	Macaca fascicularis	HMNH 37406	18.0	11.6	5.2	26.3	18.9	12.6	7.4
	Macaca fascicularis	HMNH 37407	18.3	11.9	4.5	28.4	18.6	12.4	7.4
	Macaca fascicularis	HMNH 37415	18.2	11.3	5.3	29.4	19.0	11.0	7.4
	Macaca fascicularis	HMNH 37416	18.3	11.3	5.5	28.8	18.5	11.0	7.1
	Macaca fascicularis	HMNH 57836	19.3	12.1	6.8	30.5	20.4	12.4	7.0
	Macaca mulatta	UM-APC 319	20.9	12.5	6.7	31.8	20.0	11.2	6.7
	Macaca mulatta	UM-APC 279	21.2	12.8	6.2	36.7	21.2	13.2	10.3
	Macaca mulatta	UM-APC 318	18.1	12.0	5.8	31.6	18.9	12.3	8.3
	Macaca mulatta	UM-APC 320	20.8	11.5	5.6	32.1	19.4	11.2	6.7
	Macaca mulatta	UM-APC 224	21.0	12.0	6.5	36.6	21.2	11.9	7.5
	Macaca mulatta	UM-APC 286	21.4	12.6	6.2	35.2	25.7	17.0	9.6
	Macaca mulatta	UM-APC 231	22.1	13.2	6.8	26.6	22.2	13.2	7.3
	Papio hamadryas	AMNH 200847	27.1	14.7	9.0	41.8	21.7	12.2	8.5
	Papio hamadryas	NMW 772	42.2	21.6	12.3	64.4	33.2	20.4	12.4
	Papio hamadryas	NMW 825	23.9	12.2	7.3	35.6	18.9	11.0	9.2
	Papio hamadryas	NMW 847	27.9	16.2	8.2	42.4	23.7	11.7	8.4

Supplementary Table 2. Continued

Group	Species	Key	Mc1	PP1	DP1	Mc2	PP2	IP2	DP2
	Papio hamadryas	NMW 28584	28.2	14.7	9.0	41.7	21.3	15.1	9.4
	Papio hamadryas	NMW 43411	35.1	18.1	10.3	56.0	26.4	16.0	12.2
	Papio hamadryas	NMW 22755	34.7	18.9	10.7	57.4	28.7	17.5	14.0
	Presbytis cristata	HMNH 35666	18.5	11.6	5.7	36.4	25.2	15.0	7.2
	Presbytis cristata	HMNH 35669	18.2	9.8	5.5	36.6	24.5	15.0	7.8
Cercopithecidae	*Presbytis cristata*	HMNH 35640	17.5	9.6	5.2	35.0	24.2	14.0	7.4
	Presbytis cristata	HMNH 35678	18.0	9.9	4.3	35.0	24.4	14.6	6.9
	Presbytis cristata	HMNH 35675	16.5	9.3	4.8	33.2	23.8	15.3	6.9
	Presbytis cristata	HMNH 35688	16.7	8.2	4.4	32.7	22.7	13.4	6.2
	Presbytis cristata	HMNH 35683	18.4	9.5	5.2	36.3	25.4	14.4	6.3
	Presbytis cristata	HMNH 37396	17.7	10.3	6.0	35.5	23.4	14.8	6.9
	Presbytis cristata	HMNH 37665	16.0	7.6	4.6	33.0	22.3	13.6	6.0
	Au. afarensis comp H	NME Mc1 333w-39; Mc2-5 333w-48; w-16; 56; w-89	37.8	26.0	19.0	56.9	37.4	22.3	13.7
	Au. afarensis comp P	NME Mc1 333w-39; Mc2-5 333w-48; w-16; 56; w-89	37.8	26.0	19.0	56.9	37.4	22.3	13.7
	Au. sediba MH2 H	WITS MH2	37.7	24.5	15.1	50.0	31.5	16.6	12.1
Fossils	*Au. sediba* MH2 P	WITS MH2	37.7	24.5	15.1	50.0	31.5	16.6	8.7
	Homo neanderthalensis	TAU Kebara 2	45.3	31.4	26.6	68.6	43.7	25.9	21.6
	Homo sapiens Ohalo II H2	TAU Ohalo II H2	44.0	30.8	21.7	68.0	41.3	25.6	16.9
	Homo sapiens Qafzeh 9	TAU Qafzeh 9	44.3	33.5	23.8	62.1	41.7	26.2	18.3
	Gorilla gorilla	AMNH 81652	42.4	24.1	18.4	82.6	47.4	30.1	16.7
	Gorilla gorilla	AMNH 90194	47.3	29.6	18.4	92.0	54.0	32.7	19.3
	Gorilla gorilla	ZMB 18515	49.6	30.0	23.7	93.1	55.7	37.4	16.6
	Gorilla gorilla	NMW 792	44.9	34.4	17.3	88.3	51.1	32.1	17.9
	Homo sapiens	AMNH 204072	49.8	31.3	22.6	71.7	42.2	25.7	17.2
	Homo sapiens	AMNH 172124	48.3	33.9	25.6	74.2	46.8	28.1	20.4
	Homo sapiens	WITS 1301	40.7	28.7	19.6	62.7	37.4	21.3	16.0
	Homo sapiens	WITS 1408	42.0	31.0	20.4	61.2	40.5	23.3	14.4
	Homo sapiens	WITS 1501	42.8	32.1	23.5	65.6	41.2	25.2	19.8
	Homo sapiens	WITS 1576	44.0	31.4	22.5	64.9	38.9	24.5	18.8
	Homo sapiens	WITS 1689	49.2	33.1	23.2	72.1	40.5	25.2	17.4
	Homo sapiens	WITS 1791	44.5	29.8	23.8	62.4	40.7	24.1	16.9
	Homo sapiens	WITS 1918	41.0	27.7	21.3	61.4	36.6	20.4	14.3
	Homo sapiens	WITS 1925	37.1	27.8	20.0	60.0	38.4	22.2	16.5
	Homo sapiens	WITS 1947	39.9	28.3	22.1	61.0	37.4	21.4	17.9
	Homo sapiens	WITS 2012	42.1	28.4	20.9	63.6	37.9	22.3	16.0
	Homo sapiens	WITS 2087	37.9	27.1	19.6	57.5	37.9	22.0	17.3
	Homo sapiens	WITS 2191	43.0	30.8	21.4	63.5	40.3	24.4	16.3
Hominoidea	*Homo sapiens*	WITS 3156	46.9	32.5	25.2	71.2	43.5	26.4	18.5
	Homo sapiens	WITS 3314	44.2	29.5	22.0	63.6	39.8	23.2	16.5
	Homo sapiens	WITS 3316	43.9	31.2	22.7	68.1	43.0	25.6	16.3
	Homo sapiens	WITS 3360	46.3	33.1	24.0	64.3	43.7	25.9	18.4
	Homo sapiens	WITS 3364	50.6	35.9	26.8	76.1	43.7	27.3	20.8
	Homo sapiens	WITS 3369	42.8	30.9	23.3	62.8	40.7	24.0	18.8
	Homo sapiens	WITS 3372	46.4	33.5	22.9	72.6	45.0	27.3	18.6
	Homo sapiens	WITS 3388	49.0	35.2	26.1	74.2	45.7	29.0	19.0
	Homo sapiens	WITS 3448	49.5	35.1	24.8	72.0	44.9	26.6	19.6
	Homo sapiens	WITS 3664	44.5	30.5	24.7	66.0	38.7	23.2	18.4
	Homo sapiens	WITS 3529	45.9	33.4	24.1	66.2	42.5	25.2	19.1
	Homo sapiens	WITS 3606	43.2	30.0	22.7	66.4	40.5	22.6	18.1
	Homo sapiens	WITS 178	44.0	31.5	22.9	64.4	41.8	24.6	18.4
	Homo sapiens	WITS 188	39.2	28.1	20.0	55.5	35.7	21.3	17.0
	Homo sapiens	WITS 1472	46.5	32.3	20.0	62.3	38.8	24.6	17.0
	Homo sapiens	WITS 2097	34.9	24.9	19.6	53.5	32.7	19.8	15.2
	Homo sapiens	WITS 906	44.7	29.6	22.0	63.7	38.4	22.2	17.9
	Homo sapiens	UV S22	42.5	28.2	20.1	60.6	36.5	20.9	15.6
	Homo sapiens	UV S45	37.4	25.5	17.3	57.8	34.5	18.1	13.8

Supplementary Table 2. Continued

Group	Species	Key	Mc1	PP1	DP1	Mc2	PP2	IP2	DP2
	Homo sapiens	UV S56	37.6	26.6	19.3	58.5	34.6	20.8	14.5
	Homo sapiens	UV S54	40.7	28.8	20.2	58.8	37.2	20.7	16.1
	Homo sapiens	UV S59	39.3	27.6	19.5	59.7	35.0	19.9	14.5
	Homo sapiens	UV S38	38.9	26.4	18.5	55.2	32.6	19.5	14.7
	Homo sapiens	UV S7	37.5	27.1	19.3	55.2	34.3	19.0	13.8
	Homo sapiens	UV S26	41.6	28.4	19.3	61.1	36.8	20.5	15.9
	Homo sapiens	UV S17	33.3	24.0	16.8	52.0	33.2	18.5	13.9
	Homo sapiens	UV S52	45.0	32.6	22.5	65.5	40.6	24.9	17.0
	Homo sapiens	UNI-FI 4865	47.4	35.3	24.8	71.3	46.1	27.2	19.1
	Homo sapiens	UNI-FI 4887	40.5	29.8	22.3	61.8	40.5	24.3	17.2
	Homo sapiens	UNI-FI 4868	39.0	28.7	19.2	59.1	38.6	23.9	15.5
	Homo sapiens	UNI-FI 4880	40.6	30.9	21.4	63.1	38.0	23.9	17.3
	Pan paniscus	MRAC 29052	40.6	26.1	18.7	86.2	48.9	32.4	17.4
	Pan paniscus	MRAC 29044	41.2	25.8	15.1	85.6	44.6	27.2	15.9
	Pan paniscus	MRAC 27696	39.6	25.6	15.5	87.5	48.0	30.7	15.8
	Pan paniscus	MRAC 29042	36.6	24.4	19.9	81.5	45.9	30.5	18.6
	Pan paniscus	MRAC 29045	39.0	25.7	15.9	84.2	45.2	30.1	15.2
	Pan troglodytes	AMNH 89351	34.2	23.6	19.1	81.3	46.9	30.0	15.2
	Pan troglodytes	AMNH 89353	41.0	27.8	20.9	95.7	55.6	35.2	18.5
	Pan troglodytes	AMNH 89355	37.3	27.2	18.6	81.8	48.8	30.4	15.7
Hominoidea	*Pan troglodytes*	AMNH 90189	40.5	25.8	17.6	88.4	50.0	34.3	17.8
	Pan troglodytes	HMNH 11772	31.8	22.2	16.1	71.4	41.6	27.2	13.4
	Pan troglodytes	NMW 25124	38.9	25.1	18.9	84.8	51.3	28.9	16.5
	Pan troglodytes	NMW 13528	38.0	24.0	18.3	88.4	50.0	30.3	15.9
	Pongo pygmaeus	AMNH 18010	34.3	19.2	10.2	77.6	53.1	27.3	14.4
	Pongo pygmaeus	AMNH 200898	37.8	22.8	12.8	81.0	56.4	32.6	18.2
	Pongo pygmaeus	AMNH 90395	32.5	16.6	10.2	73.9	50.8	26.2	13.1
	Pongo pygmaeus	HMNH 5154	39.2	22.7	12.8	89.1	55.7	33.3	15.8
	Pongo pygmaeus	NMW 798	51.0	31.5	7.3	100.6	74.7	42.8	25.1
	Pongo pygmaeus	NMW 795	33.9	16.7	9.1	76.8	49.1	27.7	12.0
	Pongo pygmaeus	NMW 797	37.9	23.6	7.0	85.9	52.9	31.9	15.0
	Pongo pygmaeus	NMW 800/B 5414	42.4	24.3	13.1	92.0	62.8	35.8	18.2
	Pongo pygmaeus	NMW 654	35.8	21.1	10.1	79.8	52.8	27.4	12.5
	Pongo pygmaeus	NMW 799	53.8	32.5	15.2	114.0	73.6	42.0	19.9
	Hylobates lar	HMNH 35945	31.5	16.8	9.8	58.5	38.3	24.8	10.8
	Hylobates lar	HMNH 41421	32.6	19.3	9.5	61.5	43.2	31.6	12.2
	Hylobates lar	HMNH 41476	37.3	23.3	9.3	63.3	44.0	29.7	12.2
	Hylobates lar	HMNH 41504	36.0	19.0	9.1	64.1	42.4	25.3	11.3
	Hylobates lar	HMNH 41537	30.0	18.6	9.7	52.3	36.6	24.8	12.6